

MARVEL ANALYSIS OF THE MEASURED HIGH-RESOLUTION ROVIBRONIC SPECTRA OF $^{90}\text{Zr}^{16}\text{O}$

LAURA K MCKEMMISH^{1,2}, JASMIN BORSOVSZKY², KATIE L GOODHEW³, SAMUEL SHEPPARD³, APHRA F V BENNETT³, ALFIE D J MARTIN³, AMRIK SINGH³, CALLUM A J STURGEON³, TIBOR FURTENBACHER⁴, ATTILA G. CSÁSZÁR⁴, JONATHAN TENNYSON¹

¹Department of Physics and Astronomy, University College London, London, WC1E 6BT, UK

²School of Chemistry, University of New South Wales, Kensington, Sydney, Australia

³Highams Park School, Handsworth Avenue, Highams Park, London, E4 9PJ, UK

⁴Institute of Chemistry, Loránd Eötvös University and MTA-ELTE Complex Chemical Systems Research Group, H-1518 Budapest 112, Hungary

Draft version March 7, 2022

ABSTRACT

Zirconium oxide (ZrO) is an important astrophysical molecule that defines the S-star classification class for cool giant stars. Accurate, empirical rovibronic energy levels, with associated labels and uncertainties, are reported for 9 low-lying electronic states of the diatomic $^{90}\text{Zr}^{16}\text{O}$ molecule. These 8088 empirical energy levels are determined using the MARVEL (Measured Active Rotational-Vibrational Energy Levels) algorithm with 23 317 input assigned transition frequencies, 22 549 of which were validated. A temperature-dependent partition function is presented alongside updated spectroscopic constants for the 9 low-lying electronic states.

Subject headings: molecular data; opacity; astronomical data bases: miscellaneous; planets and satellites: atmospheres; stars: low-mass.

1. INTRODUCTION

ZrO is a transition metal diatomic oxide which, like similar species, possesses strong absorption lines and a complex electronic structure. Strong ZrO absorption lines are the identifying characteristic of the rare S-type stars (Merrill 1922; Keenan 1954; Wyckoff & Clegg 1978; Ake 1979; Keenan & Boeshaar 1980; Little-Marenin & Little 1988; Van Eck & Jorissen 2000). Traditionally thought to be caused by carbon/oxygen ratios near unity (Ake 1979; Smith & Lambert 1986), the recent investigation by Van Eck et al. (2017) confirms the earlier claim by Piccirillo (1980) that the ZrO lines are caused by overabundance of s elements like Zr. Weak ZrO bands are characteristic of SC stars (Keenan & Boeshaar 1980; Zijlstra et al. 2004). Faint ZrO bands have also been identified in sun-spots (Richardson 1931; Sriramachandran & Shanmugavel 2012) and M-stars (Bobrovnikoff 1934).

The ZrO absorption bands were first observed in spectra taken by Merrill (1922), with King (1924) providing laboratory confirmation of the molecular origin of the bands. Keenan (1954) provided the first classification of S-type stars. Early studies of ZrO bands in stars include an analysis of R Geminorum by Phillips (1955).

The presence of ZrO (and other s-process elements) in S-stars is due to the nucleosynthesis s-process occurring within these stars (Joyce et al. 1998) or in a companion star before being accreted to their surface (Van Eck & Jorissen 2000). The s-process only occurs at relatively low neutron densities and intermediate temperature conditions. There are two types of S-stars depending on whether the s-process elements are formed within the star itself or transferred from a binary partner star. Short-lived cooler intrinsic S-stars are formed in around 10% of asymptotic giant branch stars when s-process elements convect to the surface due to dredge-up during the short

thermal pulse-asymptotic giant branch phase (Smith & Lambert 1985; Van Eck & Jorissen 2000). Longer-lived hotter extrinsic stars are formed due to binary system mass transfer (Lambert et al. 1995; Van Eck & Jorissen 2000), and are evolutionary understood as the descendants of barium stars (Van Eck & Jorissen 2000). They can be distinguished by the presence of Tc in intrinsic S-stars (Van Eck & Jorissen 1999; Van Eck et al. 2000; Van Eck & Jorissen 2000).

Littleton & Davis (1985) are regularly cited as providing 330,000 lines of a ZrO line list; however, these data are not available as part of the original publication. It is likely this cited line list consists of model Hamiltonian fits to the main bands along with band intensities, Franck-Condon factors and Hönl-London factors. This has been superseded by the line list using similar methods created by Plez et al. (2003), which is unpublished but freely available online. There is thus, to our knowledge, no available line list created using variational nuclear motion methods from fitted potential energy, *ab initio* dipole moment and fitted spin-orbit coupling curves, as can be constructed using current techniques by, e.g. the ExoMol group (Tennyson & Yurchenko 2017). Such studies are greatly aided by the availability of accurate empirical energy levels such as the dataset developed in this paper.

Due to its astrophysical importance, ZrO has been the subject of a large number of experimental studies. One of the aims of this paper is to review and compile the spectroscopic data from these previous studies to produce a single recommended list of experimentally derived empirical energy levels and validated transition frequencies. As part of this process, we extracted all previous experimental data into a consistent set of assigned transition frequencies with uncertainties. Future experimental results can be added to this Master List to obtain an updated list of empirical energy levels using the MARVEL pro-

gram(described below). We anticipate that these energy levels will be used to refine new spectroscopic models for $^{90}\text{Zr}^{16}\text{O}$ and produce updated extensive hot molecular line lists for use in atmospheric models.

2. METHOD

2.1. MARVEL

The Measured Active RoVibrational Energy Levels (MARVEL) approach (Furtenbacher et al. 2007; Császár et al. 2007; Furtenbacher & Császár 2012a) is an algorithm that enables a set of assigned experimental transition frequencies to be converted into empirical energy levels with associated uncertainties propagated from the input transition data to the output energy levels. This conversion relies on the construction of experimental spectroscopic networks (SNs) (Császár & Furtenbacher 2011; Furtenbacher & Császár 2012b; Furtenbacher et al. 2014; Árendás et al. 2016) which contains all interconnected transitions. For a detailed description of the approach, algorithm and program, we refer readers to Furtenbacher & Császár (2012a).

The MARVEL approach has been used to compile empirical energy levels for the very important and electronically-similar species $^{48}\text{Ti}^{16}\text{O}$ (McKemmish et al. 2017). Other MARVEL studies on astronomically important molecules include those for $^{12}\text{C}_2$ (Furtenbacher et al. 2016), acetylene (Chubb et al. 2018b), ammonia (Al Derzi et al. 2015; Furtenbacher et al. 2018), SO_2 (Tóbiás et al. 2018), H_2S (Chubb et al. 2018a) and isotopologues of H_3^+ (Furtenbacher et al. 2013b,a). These are in addition to energies for the isotopologues of water (Tennyson et al. 2009, 2010, 2013, 2014b) for which the MARVEL procedure was originally developed (Tennyson et al. 2014a).

This paper utilised the MARVEL algorithm through a specially designed web-interface, available at <http://kkrk.chem.elte.hu/marvelonline> (Furtenbacher & Császár 2018), making it highly accessible across computer systems without installation of specialised code. Numerous updates to the online interface were also made during this project and related projects in order to optimise the speed, ease and quality of data processing; for example, options were made available to automatically update uncertainties within thresholds when processing initial data to find a self-consistent spectroscopic network.

2.2. Electronic structure and spectroscopy of ZrO

ZrO and TiO share similar features in their electronic structure, as Zr is directly below Ti on the periodic table. Specifically, both have the same qualitative ordering of many low-lying electronic states (in terms of symmetry and spin), with slight differences in T_e so that, e.g. unlike in TiO, the ground electronic state of ZrO is a spin singlet, $X^1\Sigma^+$. Those states with well-characterised experimental electronic states below $25,000\text{ cm}^{-1}$ are shown in Figure 1, which also gives the observed bands linking these states. Note that we did not find any rotationally-resolved spectral data involving the $D^1\Gamma$, $E^1\Phi$, $c^3\Sigma^-$ or $f^3\Delta$ states.

The singlet $X^1\Sigma^+$ ground state has allowed excitations to the $B^1\Pi$ and $C^1\Sigma^+$ states. Significant absorption also occurs from thermal population of the $a^3\Delta$ states to the

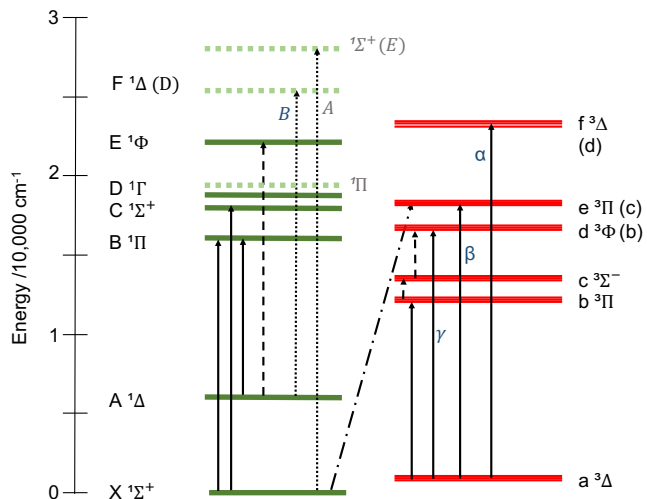


FIG. 1.— The electronic structure of $^{90}\text{Zr}^{16}\text{O}$, with approximate T_e and labels taken from Langhoff & Bauschlicher Jr (1990); where different, labels from Huber & Herzberg (1979) are given in brackets. The solid horizontal lines are those electronic states whose existence and assignment is reasonably secure with reliable theoretical predictions, while the dashed horizontal lines indicate states that some authors have proposed for ZrO but which are not supported by theory or rotationally resolved experiment. This diagram also shows the main band systems of ZrO, with solid lines showing the bands for which rotationally-resolved allowed transitions have been analysed, the alternating dotted-dashed line representing an experimentally-observed inter-combination band while long dashed lines represent allowed transitions that have not been measured in rotationally-resolved spectra and the short dashed lines represent transitions that have previously, probably erroneously, been assigned as ZrO bands.

higher singlet states $b^3\Pi$, $d^3\Phi$, $e^3\Pi$ and $f^3\Delta$. In the high temperature gaseous environments where $^{90}\text{Zr}^{16}\text{O}$ is present astrophysically, transitions from the $A^1\Delta$ state to the $B^1\Pi$ and $E^1\Phi$ states may also be relevant.

2.3. Quantum numbers and selection rules

The most obvious information to include in the label of a rovibronic state of ZrO is the electronic state, *state*, the total angular momentum, J , and the vibrational quantum number, v . We find these to be relatively unambiguous to define.

For the triplet states, we also need to provide information about the electronic spin state; in this case, we choose to include this as part of the label for the electronic state. The parity of energy levels usually only influences the energy in a measurable manner for Π states; we absorb the e and f parity labels (Brown et al. 1975) into the electronic state label to reduce the overall number of labels.

2.4. Literature Review

In the first half of the twentieth century, there was considerable interest in studying the visible and ultraviolet spectrum of $^{90}\text{Zr}^{16}\text{O}$, with many bandheads measured by Lowater (1932), Herbig (1949), Afaf (1949), Afaf (1950a) and Afaf (1950b). These studies include many involving transitions to electronic states that have yet to be investigated using rotationally-resolved spectra.

More recently, there was an extensive experimental effort over the 1970s to early 1980s by various groups to

obtain rotationally resolved assigned experimental spectra for various important $^{90}\text{Zr}^{16}\text{O}$ bands; these studies as well as more recent rotationally resolved studies are summarized in Table 1.

Two further studies in the 1980s, Hammer et al. (1981)

and Stepanov et al. (1988), investigated higher vibrational levels of some of the most important electronic states but without rotational resolution.

TABLE 1 – DATA SOURCES AND THEIR CHARACTERISTICS FOR $^{90}\text{Zr}^{16}\text{O}$. A/V MEANS AVAILABLE/VALIDATED.

Tag	Ref	Band	Range(cm^{-1})	J Range	Trans. (A/V)	Uncertainties (cm^{-1})			
						Min	Av	Max	
54LaUhBa	Lagerqvist et al. (1954)	d $^3\Phi_2$ – a $^3\Delta_1$	0 - 0	15282 - 15442	11 - 89	159/159	0.1	0.1	0.28
		d $^3\Phi_3$ – a $^3\Delta_2$	0 - 0	15612 - 15755	11 - 93	149/149	0.1	0.1	0.32
		d $^3\Phi_4$ – a $^3\Delta_3$	0 - 0	15898 - 16048	11 - 95	165/165	0.1	0.11	0.34
		f $^3\Delta_1$ – a $^3\Delta_1$	0 - 0	21351 - 21542	20 - 76	105/105	0.1	0.1	0.31
		f $^3\Delta_2$ – a $^3\Delta_2$	0 - 0	21351 - 21555	20 - 80	111/111	0.1	0.1	0.1
		f $^3\Delta_3$ – a $^3\Delta_3$	0 - 0	21457 - 21640	20 - 81	106/106	0.1	0.1	0.1
54Uhler	Uhler (1954b)	e $^3\Pi_{0e}$ – a $^3\Delta_1$	0 - 0	17884 - 18002	15 - 60	106/106	0.1	0.1	0.14
		e $^3\Pi_{0f}$ – a $^3\Delta_1$	0 - 0	17889 - 18006	27 - 59	96/91	0.1	0.1	0.3
		e $^3\Pi_{1e}$ – a $^3\Delta_2$	0 - 0	17619 - 17757	20 - 74	103/91	0.1	0.12	0.31
		e $^3\Pi_{1f}$ – a $^3\Delta_2$	0 - 0	17653 - 17758	19 - 59	99/63	0.1	0.19	0.62
		e $^3\Pi_2$ – a $^3\Delta_3$	0 - 0	17326 - 17483	13 - 85	143/139	0.1	0.15	0.43
57Akerlind	Akerlind (1957)	F $^1\Delta$ – A $^1\Delta$	0 - 0	18994 - 19280	17 - 102	156/156	0.1	0.1	0.11
		F $^1\Delta$ – A $^1\Delta$	1 - 0	19843 - 20106	35 - 94	110/110	0.1	0.1	0.15
73BaTa	Balfour & Tatum (1973)	B $^1\Pi_e$ – X $^1\Sigma^+$	0 - 0	15136 - 15391	18 - 107	149/145	0.01	0.031	0.16
		B $^1\Pi_f$ – X $^1\Sigma^+$	0 - 0	15185 - 15382	8 - 96	85/83	0.01	0.024	0.13
73Lindgren	Lindgren (1973)	e $^3\Pi_{1e}$ – a $^3\Delta_1$	0 - 0	17995 - 18050	30 - 61	53/53	0.07	0.086	0.19
		e $^3\Pi_{1f}$ – a $^3\Delta_1$	0 - 0	17991 - 18048	30 - 60	51/50	0.07	0.09	0.23
		e $^3\Pi_2$ – a $^3\Delta_2$	0 - 0	17761 - 17820	47 - 65	36/29	0.07	0.12	0.35
76PhDa.CX	Phillips & Davis (1976a)	C $^1\Sigma^+$ – X $^1\Sigma^+$	0 - 0	16732 - 17060	2 - 121	232/203	0.02	0.044	0.19
76PhDa.BX	Phillips & Davis (1976b)	B $^1\Pi_e$ – X $^1\Sigma^+$	0 - 0	15102 - 15391	5 - 132	201/188	0.02	0.039	0.14
		B $^1\Pi_e$ – X $^1\Sigma^+$	0 - 1	14292 - 14423	1 - 102	144/135	0.02	0.046	0.18
		B $^1\Pi_e$ – X $^1\Sigma^+$	0 - 2	13244 - 13431	17 - 116	101/100	0.02	0.042	0.1
		B $^1\Pi_e$ – X $^1\Sigma^+$	1 - 0	16023 - 16244	1 - 107	149/148	0.02	0.046	0.16
		B $^1\Pi_e$ – X $^1\Sigma^+$	1 - 2	14038 - 14313	4 - 116	177/175	0.02	0.045	0.31
		B $^1\Pi_e$ – X $^1\Sigma^+$	1 - 3	13246 - 13359	1 - 102	135/134	0.02	0.042	0.15
		B $^1\Pi_e$ – X $^1\Sigma^+$	2 - 0	16817 - 17091	4 - 117	159/142	0.02	0.056	0.2
		B $^1\Pi_e$ – X $^1\Sigma^+$	2 - 1	15936 - 16122	1 - 104	146/136	0.02	0.046	0.27
		B $^1\Pi_e$ – X $^1\Sigma^+$	2 - 3	14046 - 14205	1 - 106	136/135	0.02	0.048	0.17
		B $^1\Pi_e$ – X $^1\Sigma^+$	2 - 4	13122 - 13257	2 - 108	150/147	0.02	0.034	0.14
		B $^1\Pi_e$ – X $^1\Sigma^+$	3 - 1	16690 - 16963	1 - 90	114/111	0.02	0.038	0.14
		B $^1\Pi_e$ – X $^1\Sigma^+$	3 - 5	13051 - 13157	1 - 100	135/132	0.02	0.036	0.24
		B $^1\Pi_e$ – X $^1\Sigma^+$	3 - 6	11990 - 12223	1 - 136	188/185	0.02	0.036	0.15
		B $^1\Pi_e$ – X $^1\Sigma^+$	4 - 2	16547 - 16836	2 - 116	139/139	0.02	0.04	0.3
		B $^1\Pi_e$ – X $^1\Sigma^+$	4 - 5	13746 - 13991	1 - 104	102/100	0.02	0.043	0.3
		B $^1\Pi_e$ – X $^1\Sigma^+$	4 - 6	12824 - 13057	2 - 108	132/132	0.02	0.042	0.22
		B $^1\Pi_e$ – X $^1\Sigma^+$	5 - 3	16659 - 16710	2 - 61	46/46	0.02	0.029	0.064
		B $^1\Pi_e$ – X $^1\Sigma^+$	5 - 7	12822 - 12959	2 - 108	130/130	0.02	0.026	0.13
		B $^1\Pi_f$ – X $^1\Sigma^+$	0 - 0	15108 - 15383	1 - 113	114/109	0.02	0.036	0.17
		B $^1\Pi_f$ – X $^1\Sigma^+$	0 - 1	14289 - 14414	2 - 80	77/73	0.02	0.047	0.44
		B $^1\Pi_f$ – X $^1\Sigma^+$	0 - 2	13250 - 13431	34 - 107	70/70	0.02	0.034	0.14
		B $^1\Pi_f$ – X $^1\Sigma^+$	1 - 0	16021 - 16237	1 - 96	93/93	0.02	0.037	0.1
		B $^1\Pi_f$ – X $^1\Sigma^+$	1 - 3	13248 - 13349	3 - 76	72/72	0.02	0.036	0.16
		B $^1\Pi_f$ – X $^1\Sigma^+$	2 - 0	16759 - 17084	2 - 113	96/94	0.02	0.046	0.2
		B $^1\Pi_f$ – X $^1\Sigma^+$	2 - 1	15938 - 16115	3 - 87	81/76	0.02	0.04	0.19
		B $^1\Pi_f$ – X $^1\Sigma^+$	2 - 3	14039 - 14195	9 - 90	72/72	0.02	0.04	0.15
		B $^1\Pi_f$ – X $^1\Sigma^+$	2 - 4	13122 - 13248	1 - 85	80/77	0.02	0.033	0.097
		B $^1\Pi_f$ – X $^1\Sigma^+$	3 - 1	16703 - 16957	1 - 100	90/87	0.02	0.04	0.19
		B $^1\Pi_f$ – X $^1\Sigma^+$	3 - 5	13050 - 13148	2 - 75	69/68	0.02	0.035	0.2
		B $^1\Pi_f$ – X $^1\Sigma^+$	3 - 6	11986 - 12213	3 - 121	99/97	0.02	0.033	0.11
		B $^1\Pi_f$ – X $^1\Sigma^+$	4 - 2	16555 - 16830	1 - 104	81/79	0.02	0.037	0.19
		B $^1\Pi_f$ – X $^1\Sigma^+$	4 - 5	13748 - 13983	1 - 110	74/73	0.02	0.033	0.19
		B $^1\Pi_f$ – X $^1\Sigma^+$	4 - 6	12834 - 13047	8 - 111	96/96	0.02	0.035	0.19
		B $^1\Pi_f$ – X $^1\Sigma^+$	5 - 3	16661 - 16704	3 - 41	30/30	0.02	0.025	0.06
		B $^1\Pi_f$ – X $^1\Sigma^+$	5 - 7	12822 - 12950	1 - 86	77/77	0.02	0.022	0.06

Continued on next page

TABLE 1 – continued from previous page

Tag	Ref	Band	Range(cm ⁻¹)	J Range	Trans.(A/V)	Uncertainties (cm ⁻¹)			
						Min	Av	Max	
79GaDe	Gallaher & Devore (1979)	X ¹ Σ ⁺ – X ¹ Σ ⁺	1 - 0	952 - 986	1 - 20	40/33	0.02	0.075	0.42
79PhDa	Phillips & Davis (1979a)	d ³ Φ ₂ – a ³ Δ ₁	0 - 0	15132 - 15442	2 - 150	372/371	0.02	0.037	0.14
		d ³ Φ ₂ – a ³ Δ ₁	0 - 1	14172 - 14515	2 - 150	351/350	0.02	0.042	0.13
		d ³ Φ ₂ – a ³ Δ ₁	1 - 0	15862 - 16289	2 - 151	393/393	0.02	0.04	0.14
		d ³ Φ ₂ – a ³ Δ ₁	1 - 1	15089 - 15361	2 - 150	327/318	0.02	0.046	0.2
		d ³ Φ ₂ – a ³ Δ ₁	1 - 2	14093 - 14440	2 - 151	358/357	0.02	0.041	0.16
		d ³ Φ ₂ – a ³ Δ ₁	2 - 1	15814 - 16191	3 - 151	356/355	0.02	0.047	0.17
		d ³ Φ ₂ – a ³ Δ ₁	2 - 2	14928 - 15277	1 - 149	327/314	0.02	0.046	0.2
		d ³ Φ ₂ – a ³ Δ ₁	2 - 3	14015 - 14364	2 - 151	363/362	0.02	0.045	0.17
		d ³ Φ ₂ – a ³ Δ ₁	3 - 2	15679 - 16113	2 - 151	411/407	0.02	0.049	0.2
		d ³ Φ ₂ – a ³ Δ ₁	3 - 3	14929 - 15194	2 - 137	332/329	0.02	0.039	0.12
		d ³ Φ ₂ – a ³ Δ ₁	3 - 4	13944 - 14289	3 - 151	371/370	0.02	0.038	0.17
		d ³ Φ ₂ – a ³ Δ ₁	3 - 5	13214 - 13384	2 - 101	206/206	0.02	0.051	0.14
		d ³ Φ ₂ – a ³ Δ ₁	4 - 3	15802 - 16024	2 - 101	261/261	0.02	0.041	0.13
		d ³ Φ ₂ – a ³ Δ ₁	4 - 5	13877 - 14214	2 - 151	348/348	0.02	0.039	0.18
		d ³ Φ ₂ – a ³ Δ ₁	5 - 6	13947 - 14136	2 - 101	209/209	0.02	0.023	0.13
		d ³ Φ ₃ – a ³ Δ ₂	0 - 0	15417 - 15754	2 - 144	375/361	0.02	0.033	0.2
		d ³ Φ ₃ – a ³ Δ ₂	0 - 1	14499 - 14675	83 - 150	83/77	0.02	0.052	0.18
		d ³ Φ ₃ – a ³ Δ ₂	1 - 0	16163 - 16602	2 - 150	397/395	0.02	0.036	0.53
		d ³ Φ ₃ – a ³ Δ ₂	1 - 1	15423 - 15665	1 - 133	307/291	0.02	0.037	0.17
		d ³ Φ ₃ – a ³ Δ ₂	1 - 2	14490 - 14749	2 - 151	363/358	0.02	0.037	0.2
		d ³ Φ ₃ – a ³ Δ ₂	2 - 1	16065 - 16514	2 - 151	375/361	0.02	0.037	0.29
		d ³ Φ ₃ – a ³ Δ ₂	2 - 2	15198 - 15591	1 - 147	374/353	0.02	0.049	0.2
		d ³ Φ ₃ – a ³ Δ ₂	2 - 3	14309 - 14673	2 - 151	365/336	0.02	0.041	0.17
		d ³ Φ ₃ – a ³ Δ ₂	3 - 2	15972 - 16422	2 - 151	387/353	0.02	0.047	0.2
		d ³ Φ ₃ – a ³ Δ ₂	3 - 3	15102 - 15508	2 - 151	358/333	0.02	0.053	0.24
		d ³ Φ ₃ – a ³ Δ ₂	3 - 4	14230 - 14594	3 - 150	308/303	0.02	0.031	0.19
		d ³ Φ ₃ – a ³ Δ ₂	3 - 5	13516 - 13696	2 - 101	178/177	0.02	0.043	0.15
		d ³ Φ ₃ – a ³ Δ ₂	4 - 3	16103 - 16335	2 - 101	244/244	0.02	0.037	0.13
		d ³ Φ ₃ – a ³ Δ ₂	4 - 5	14150 - 14518	3 - 151	336/336	0.02	0.038	0.2
		d ³ Φ ₃ – a ³ Δ ₂	5 - 6	14250 - 14445	2 - 101	222/222	0.02	0.024	0.081
		d ³ Φ ₄ – a ³ Δ ₃	0 - 0	15704 - 16040	3 - 151	360/330	0.02	0.053	0.23
		d ³ Φ ₄ – a ³ Δ ₃	0 - 1	14833 - 15117	3 - 151	370/350	0.02	0.04	0.19
		d ³ Φ ₄ – a ³ Δ ₃	1 - 0	16488 - 16898	3 - 147	363/348	0.02	0.045	0.24
		d ³ Φ ₄ – a ³ Δ ₃	1 - 1	15666 - 15967	3 - 150	336/321	0.02	0.053	0.2
		d ³ Φ ₄ – a ³ Δ ₃	1 - 2	14686 - 15042	4 - 151	395/382	0.02	0.042	0.17
		d ³ Φ ₄ – a ³ Δ ₃	2 - 1	16358 - 16809	3 - 151	403/397	0.02	0.044	0.2
d ³ Φ ₄ – a ³ Δ ₃	2 - 2	15604 - 15885	3 - 147	311/298	0.02	0.059	0.2		
d ³ Φ ₄ – a ³ Δ ₃	2 - 3	14667 - 14970	3 - 136	372/365	0.02	0.038	0.18		
d ³ Φ ₄ – a ³ Δ ₃	3 - 2	16270 - 16724	3 - 151	393/386	0.02	0.045	0.2		
d ³ Φ ₄ – a ³ Δ ₃	3 - 3	15566 - 15796	3 - 108	239/237	0.02	0.049	0.17		
d ³ Φ ₄ – a ³ Δ ₃	3 - 4	14685 - 14897	3 - 105	262/262	0.02	0.034	0.18		
d ³ Φ ₄ – a ³ Δ ₃	3 - 5	13813 - 13991	3 - 101	187/186	0.02	0.045	0.15		
d ³ Φ ₄ – a ³ Δ ₃	4 - 3	16410 - 16636	3 - 101	251/250	0.02	0.045	0.16		
d ³ Φ ₄ – a ³ Δ ₃	4 - 5	14469 - 14824	3 - 151	385/385	0.02	0.031	0.16		
d ³ Φ ₄ – a ³ Δ ₃	5 - 6	14558 - 14752	3 - 101	224/224	0.02	0.023	0.11		
80HaDa	Hammer & Davis (1980)	e ³ Π _{1e} – X ¹ Σ ⁺	0 - 0	19047 - 19121	29 - 41	24/23	0.01	0.025	0.085
		e ³ Π _{1e} – X ¹ Σ ⁺	0 - 1	18094 - 18152	32 - 39	8/6	0.01	0.032	0.071
		e ³ Π _{1e} – a ³ Δ ₂	0 - 0	17693 - 17735	30 - 41	22/21	0.01	0.024	0.097
		e ³ Π _{1f} – X ¹ Σ ⁺	0 - 0	19085 - 19095	29 - 37	9/9	0.01	0.022	0.042
		e ³ Π _{1f} – X ¹ Σ ⁺	0 - 1	18120 - 18128	29 - 35	7/6	0.01	0.012	0.015
		e ³ Π _{1f} – a ³ Δ ₂	0 - 0	17695 - 17736	26 - 41	28/26	0.01	0.022	0.081
81HaDa	Hammer & Davis (1981)	B ¹ Π _e – A ¹ Δ	0 - 0	9102 - 9507	2 - 147	394/354	0.01	0.017	0.14
		B ¹ Π _e – A ¹ Δ	1 - 0	10057 - 10359	3 - 109	176/176	0.01	0.024	0.13
		B ¹ Π _e – A ¹ Δ	2 - 1	10022 - 10271	3 - 115	151/149	0.01	0.023	0.17
		B ¹ Π _f – A ¹ Δ	0 - 0	9152 - 9507	2 - 149	373/336	0.01	0.016	0.09
		B ¹ Π _f – A ¹ Δ	1 - 0	10110 - 10359	3 - 118	179/178	0.01	0.021	0.12
		B ¹ Π _f – A ¹ Δ	2 - 1	10033 - 10271	3 - 115	159/155	0.01	0.022	0.13
81HaDaZo	Hammer et al. (1981)	B ¹ Π _e – A ¹ Δ	1 - 0	10324 - 10359	14 - 22	21/21	0.01	0.011	0.02
		B ¹ Π _e – a ³ Δ	1 - 1	13915 - 13948	15 - 21	11/11	0.01	0.01	0.01
88SiMiHuHa	Simard et al. (1988b)	C ¹ Σ ⁺ – X ¹ Σ ⁺	0 - 0	17011 - 17060	0 - 30	59/57	0.006	0.025	0.1
90SuLoFrMa	Suenram et al. (1990)	X ¹ Σ ⁺ – X ¹ Σ ⁺	0 - 0	0 - 1	0 - 1	1/1	3×10 ⁻⁷	3×10 ⁻⁷	3×10 ⁻⁷
94Jonsson	Jonsson (1994)	b ³ Π _{0e} – a ³ Δ ₁	0 - 0	10535 - 10714	7 - 107	180/180	0.006	0.012	0.069

Continued on next page

TABLE 1 – continued from previous page

Tag	Ref	Band	Range(cm ⁻¹)	<i>J</i> Range	Trans.(A/V)	Uncertainties (cm ⁻¹)			
						Min	Av	Max	
		b ³ Π _{0f} – a ³ Δ ₁	0 - 0	10579 - 10702	14 - 92	113/113	0.006	0.0078	0.026
		b ³ Π _{1e} – a ³ Δ ₂	0 - 0	10611 - 10728	11 - 100	137/137	0.006	0.0088	0.045
		b ³ Π _{1f} – a ³ Δ ₂	0 - 0	10625 - 10731	20 - 90	104/104	0.006	0.0097	0.067
		b ³ Π _{2e} – a ³ Δ ₃	0 - 0	10614 - 10750	11 - 111	171/171	0.006	0.0075	0.049
		b ³ Π _{2f} – a ³ Δ ₃	0 - 0	10614 - 10750	11 - 111	168/168	0.006	0.0079	0.049
95KaMcHe	Kaledin et al. (1995)	e ³ Π _{1e} – a ³ Δ ₁	0 - 0	17993 - 18050	2 - 63	67/66	0.007	0.013	0.057
		e ³ Π _{1f} – a ³ Δ ₁	0 - 0	17984 - 18048	2 - 67	79/79	0.007	0.016	0.084
		e ³ Π ₂ – a ³ Δ ₂	0 - 0	17748 - 17820	2 - 64	95/92	0.007	0.021	0.31
99BeGe	Beaton & Gerry (1999)	X ¹ Σ ⁺ – X ¹ Σ ⁺	0 - 0	1 - 1	0 - 1	1/1	1×10 ⁻⁷	1×10 ⁻⁷	1×10 ⁻⁷
		X ¹ Σ ⁺ – X ¹ Σ ⁺	1 - 1	0 - 1	0 - 1	1/1	1×10 ⁻⁷	1×10 ⁻⁷	1×10 ⁻⁷
		X ¹ Σ ⁺ – X ¹ Σ ⁺	2 - 2	0 - 1	0 - 1	1/1	1×10 ⁻⁷	1×10 ⁻⁷	1×10 ⁻⁷
		X ¹ Σ ⁺ – X ¹ Σ ⁺	3 - 3	0 - 1	0 - 1	1/1	1×10 ⁻⁷	1×10 ⁻⁷	1×10 ⁻⁷

Beyond the wavenumber of the lines, many experimental studies have focused on the intensity of transitions, e.g. (Herbig 1949; Murthy & Prahllad 1980; Littleton & Davis 1985; Littleton et al. 1993), radiative lifetimes, e.g. (Hammer 1978; Hammer & Davis 1979; Simard et al. 1988b) and permanent dipole moments, e.g. (Suenram et al. 1990; Pettersson et al. 2000).

The partition function and dissociation constants for zirconium oxide have been considered by various authors, including Shankar & Littleton (1983).

There are a number of other studies of ZrO spectra which we have not used in this study for various reasons. These data sources are collated in Table 2 with brief comments.

The data in Tatum & Balfour (1973) was of very poor readability, which meant the accuracy of digitisation even manually could not be guaranteed. As there are substantial more modern data available for the same transitions, we did not use these data.

A key omission to our MARVEL collation is the Phillips et al. (1979) paper; the subsequent study by Jonsson (1994) performed a complete re-analysis of the ZrO spectra in the region around 10,750 cm⁻¹ that assigned all bands whereas the Phillips et al. (1979) analysis omitted many bands. A key feature of the Jonsson (1994) analysis was a large Λ-doubling splitting between the b ³Π_{0e} and the b ³Π_{0f} state. This is attributed to spin-orbit coupling with the nearby c ³Σ⁻ state whose *T_e* was only predicted semi-quantitatively with computational techniques in the 1990s.

Unfortunately, the data of Simard et al. (1988a) could not be located; however, the spectra and analysis by Kaledin et al. (1995) covers the same spectral transitions.

Finally, we want to briefly discuss Balfour & Chowdhury (2010) in more detail, particularly their claim to observe a ¹Π – X ¹Σ⁺ system near 19,480 cm⁻¹. We strongly question this assignment because there is no expectation of a ¹Π state in this energy range from either *ab initio* calculations or analogy to the TiO electronic states. Based on vibrational frequencies, the spectrum they observe does not appear to come from overtones of a B ¹Π–X ¹Σ⁺ band. The only experimental reference to a ¹Π state in this energy range is from Simard et al. (1988a) who explain perturbation in the e ³Π triplet splittings using a ¹Π state originally predicted theoreti-

cally by Green (1969). The energies of electronic states in this energy range for transition metal diatomics are notoriously challenging to predict accurately even with today’s methods (Tennyson et al. 2016) and thus this early theoretical investigation cannot be trusted even qualitatively for higher electronic states, especially since more recent theoretical papers (Langhoff & Bauschlicher Jr 1990) make no such predictions for a ¹Π state in this energy range.

Attempts to assign the clearly visible bands seen by Balfour & Chowdhury (2010) to a ⁹⁰Zr¹⁶O transition were unconvincing. Given the low resolution of these data and its inconsistencies with current knowledge of the electronic structure of ZrO from both a theoretical and experimental perspective, we suggest these unassigned peaks are due to ZrO⁺. The method used by Balfour & Chowdhury (2010) does involve the creation of ions, and there is precedence for this occurring. Phillips & Davis (1979b) conducted a study on bands in what was understood to be the ZrO spectrum with heads at 7811 and 8192 Å that had previously been observed by Afaf (1950a) and analysed by Uhler & Åkerlind (1955) and Uhler & Åkerlind (1956) as belonging to a new system. They found these bands belonged to a ²Π – ²Σ system of ZrO⁺. While further work has been done on ZrO⁺, none of these studies have examined the same wavelengths as Balfour & Chowdhury (2010), and thus no definitive assignment can be made at this stage.

We do not extensively review the theoretical literature, but notable calculations include those of Langhoff & Bauschlicher Jr (1988), Langhoff & Bauschlicher Jr (1990) and Shanmugavel & Sriramachandran (2011).

2.5. Rotationally-resolved data sources

Our analysis started by digitising available assigned rovibronic transitions data, then converting them to MARVEL format. The full list of compiled data converted to MARVEL format is given in the Supplementary Information; an extract is given in Table 3. The full list of data sources used in the rotationally-resolved MARVEL analysis are summarised in Table 1; we provide information on the vibronic bands measured, the wavenumber range and *J* range, as well as the number of transitions measured. In total, we use 12 data sources, involving 9 electronic states with 23 317 transitions and 72 total unique spin-vibronic bands (ignoring Λ splitting).

TABLE 2
EXPERIMENTAL ZRO PAPERS NOT USED IN THE ROTATIONALLY-RESOLVED MARVEL OR BANDHEAD ANALYSIS.

Ref	Comment
Lowater (1935)	Good analysis of vibronic bands (including triplet splitting), but the rotational analysis of the $f^3\Delta - a^3\Delta$ is incorrect.
Tanaka & Horie (1941)	Incorrect rotational analysis of the $b^3\Pi - a^3\Delta$ bands and more recent data are available
Kiess (1948)	Data not available online.
Herbig (1949)	Unassigned.
Uhler (1954a)	Rotational analysis with band constants, but assigned line positions are given in the associated papers (Lagerqvist et al. 1954; Uhler 1954b).
Uhler & Åkerlind (1955)	Rotational analysis with band constants for singlet A system, but assigned line positions are given in the associated paper (Uhler & Åkerlind 1956)
Åkerlind (1956)	Band constants from analysis of a system assigned as the singlet B system at 8192 Å, but this is not consistent with Åkerlind (1957).
Åkerlind (1957)	Rotationally-resolved data from a system assigned as the singlet B system, but with frequencies around 19,000 cm^{-1} , not 12,000 cm^{-1} as indicated by the 8192 Å labelling. Due to this confusion, and some later papers (Phillips & Davis 1979b; Balfour & Lindgren 1980) that provide good evidence that the 8192 Å band (around 12,000 cm^{-1}) is a ZrO^+ band, these data are not included in our compilation.
Tatum & Balfour (1973)	Data very poorly reproduced digitally, and higher resolution spectra for the $d^3\Phi - a^3\Delta$ bands studied are available.
Weltner & McLeod (1965)	Ground state determination in Ne matrix.
Schoonveld & Sundaram (1974)	Complete and systematic analysis of available data for triplet systems, but provides no assigned rotationally resolved data.
Bijc et al. (1974)	Determination of Singlet-Triplet separation, but no assigned rotational data.
Lauchlan et al. (1976)	ZrO in Ne inert matrix at 4K
Phillips et al. (1979)	The rotational analysis here was shown to be incorrect by the subsequent re-analysis by Jonsson (1994); see text.
Gallaher & Devore (1979)	Rotationally unresolved infrared study; used for comparison against bandheads but not as part of the MARVEL dataset.
Murty (1980b)	Contains molecular constants for $e^3\Pi$ and $c^3\Sigma^-$, but provides no assigned rotationally resolved data.
Hammer et al. (1981)	Identification of bands in astronomical vs. laboratory spectra, not rotational analysis.
Afaf (1987)	Reanalysis of data and recommended molecular constants; also proposes a singlet C band from $X^1\Sigma^+$ to a singlet at 7870 cm^{-1} above; this was later discounted (e.g. Afaf (1995)).
Davis & Hammer (1988)	Consolidation of data and proposed electronic structure.
Simard et al. (1988a)	High resolution study of the $e^3\Pi - a^3\Delta$ 0-0 band; assigned line positions were not published with the original data and could not be located.
Afaf (1995)	Discusses the $\delta(^3\Pi - a^3\Delta)$ and $\phi(^3\Delta - a^3\Delta)$ bands, but provides no assigned rotationally resolved data.
Balfour & Chowdhury (2010)	Low resolution data with bandhead information on the $C^1\Sigma^+ - X^1\Sigma^+$ state.

TABLE 3
EXTRACT FROM THE 90ZR-16O.MARVEL.INP INPUT FILE FOR $^{90}\text{Zr}^{16}\text{O}$.

1	2	3	4	5	6	7	8	9
$\tilde{\nu}$	$\Delta\tilde{\nu}$	State'	v'	J'	State''	v''	J''	ID
17059.5189	0.006000	C1Sigma+	0	18	X1Sigma+	0	17	88SiMiHuHa.46
17059.9101	0.006000	C1Sigma+	0	21	X1Sigma+	0	20	88SiMiHuHa.49
17059.9295	0.006000	C1Sigma+	0	25	X1Sigma+	0	24	88SiMiHuHa.53
17059.9792	0.006000	C1Sigma+	0	24	X1Sigma+	0	23	88SiMiHuHa.52
10710.4902	0.006622	b3Pi.2e	0	46	a3Delta.3	0	46	94Jonsson.540
10710.4902	0.006622	b3Pi.2f	0	46	a3Delta.3	0	46	94Jonsson.730
10617.7781	0.006660	b3Pi.2e	0	79	a3Delta.3	0	80	94Jonsson.690

Column	Notation	
1	$\tilde{\nu}$	Transition frequency (in cm^{-1})
2	$\Delta\tilde{\nu}$	Estimated uncertainty in transition frequency (in cm^{-1})
3	State'	Electronic state of upper energy level; also includes parity for Π states and Ω for triplet states
4	v'	Vibrational quantum number of upper level
5	J'	Total angular momentum of upper level
6	State''	Electronic state of lower energy level; also includes parity for Π states and Ω for triplet states
7	v''	Vibrational quantum number of lower level
8	J''	Total angular momentum of lower level
9	ID	Unique ID for transition, with reference key for source (see Table 1) and counting number

Comments related to Table 1, particularly regarding the initial uncertainty chosen for the data, are as follows:

54LaUhBa: An uncertainty of 0.1 cm^{-1} was chosen, enabling a high number of validated transitions within this dataset and those by the same author in the same year.

54Uhler: Uncertainty as for 54LaUhBa, though this data set could be compared against later data more directly and thus had a bigger influence on setting the maximum uncertainty used.

56UhaK: Uncertainty as for 54LaUhBa. The symmetry of the two electronic states was not confirmed at the time of publication, but both can now be assigned as $^1\Sigma^+$, given the later assignment of the ground state symmetry as $^1\Sigma^+$ and the lack of a Q branch.

57Akerlind: Uncertainty as for 54LaUhBa; this data were the only source of F $^1\Delta$ state information, so uncertainty reflects only requirements for self-consistency within this data set.

73BaTa: The data table has poor readability and it is likely that minor errors in digitisation may exist, though major errors were corrected by hand using the systematic nature of the transition frequencies. We adopted 0.01 cm^{-1} as the minimum uncertainty for the data (with higher values adopted as necessary up to 0.16 cm^{-1}), as this yielded a reasonable number of self-consistent results.

73Lindgren: No uncertainty is stated in the paper; however, 0.07 cm^{-1} gave reasonable self-consistent calculations for most bands. Note that these are satellite bands and hence had lower intensities and higher position uncertainties than for the main bands.

76PhDa.BX, 76PhDa.CX: The original paper did not use the C $^1\Sigma^+$ label for the upper state; this has been named in subsequent discussions of $^{90}\text{Zr}^{16}\text{O}$ and adopted here. There are no uncertainties given; however, we found that at least 0.02 cm^{-1} was required to enable a significant number of this data to self validate. Some data were substantially more inaccurate than this; we have removed all data that required uncertainties of more than 0.2 cm^{-1} to be consistent with the rest of the data.

79PhDa: Data obtained from Kurucz and given uncertainties of 0.02 cm^{-1} , as for other Phillips and Davis data of this era. The d $^3\Phi_3 - a^3\Delta_2(0-1)$ band appears to be largely incorrectly assigned; we have used only those transitions that agree well with assignments from other bands.

80HaDa, 81HaDaZo, 81HaDa: 0.01 cm^{-1} was stated as the measurement accuracy for at least some bands; this was adopted for the whole data set by multiple papers by the same authors in similar time period. Note that this is a factor of two more accurate than earlier data from Davis and co-workers.

TABLE 4
EXTRACT FROM THE 90ZR-16O.MAIN.ENERGIES OUTPUT FILE FOR $^{90}\text{Zr}^{16}\text{O}$. ENERGIES AND THEIR UNCERTAINTIES ARE GIVEN IN CM^{-1} . NO INDICATES THE NUMBER OF TRANSITIONS WHICH CONTRIBUTED TO THE STATED ENERGY AND UNCERTAINTY.

State	v	J	\tilde{E}	Unc.	No
X1Sigma+	5	92	8286.730593	0.016290	3
a3Delta.1	4	93	8289.132156	0.013142	3
a3Delta.2	4	89	8295.024932	0.018098	3
X1Sigma+	6	79	8296.993918	0.009580	6
a3Delta.1	1	124	8312.622601	0.022336	7
A1Delta	0	76	8313.129649	0.004368	11
a3Delta.2	5	76	8320.754165	0.013995	5
a3Delta.2	3	101	8322.052377	0.013804	6
a3Delta.2	1	121	8322.707720	0.012197	7
X1Sigma+	4	104	8327.541550	0.020000	1
A1Delta	1	60	8336.081220	0.008485	2
a3Delta.2	0	130	8336.647124	0.013307	6

88SiMiHuHa: The stated uncertainty was 200 MHz, with reproducibility to 50 MHz; we therefore adopted 0.006 cm^{-1} as an initial uncertainty for our data.

90SuLoFrMa: The stated uncertainty was 4 kHz ($3 \times 10^{-8} \text{ cm}^{-1}$); however, consistency with 99BeGe required an uncertainty estimate of $3 \times 10^{-7} \text{ cm}^{-1}$.

95Jonsson: The stated uncertainty was 0.016 cm^{-1} ; however, we found a smaller uncertainty of 0.006 cm^{-1} as an initial estimate was warranted due to the consistency of the data both internally and with other results.

95KaMcHe: The stated uncertainty was 0.03 cm^{-1} ; however, we found a smaller uncertainty of 0.007 cm^{-1} as an initial estimate was warranted due to the consistency of the data both internally and with other results.

99BeGe: The stated uncertainty was 1 kHz (10^{-8} cm^{-1}); however, consistency with 90SuLoFrMa required uncertainty of 10^{-7} cm^{-1} , so this was adopted for all values.

During the MARVEL process, many of our initial estimated uncertainties were updated to establish a self-consistent network, while some transitions were removed from consideration (designated through a minus sign at the start of the MARVEL input line for that transition). To assess the data, Table 1 provides data on the minimum, average and maximum uncertainty of each transition; in most cases, we were able to keep the minimum and average uncertainty to within a factor of two. We validated 22 549 of our 23 317 input transitions, i.e. showed that these validated transitions were consistent with other measurements. The $^{90}\text{Zr}^{16}\text{O}$ MARVEL input file can readily be updated in the future with new spectroscopic information to enable an updated set of MARVEL energies to be created.

TABLE 5 SPECTROSCOPIC NETWORK CONTAINING 8088 ENERGY LEVELS AND THEIR CHARACTERISTICS FOR $^{90}\text{Zr}^{16}\text{O}$

	v	J Range	Uncertainties (cm^{-1})		
			Min	Av	Max
X $^1\Sigma^+$	0	0 - 131	1×10^{-7}	0.0096	0.055
	1	2 - 107	0.006	0.016	0.08
	2	2 - 115	0.0079	0.016	0.11
	3	2 - 105	0.008	0.014	0.052
	4	2 - 106	0.012	0.02	0.068
	5	2 - 107	0.0089	0.015	0.051
	6	2 - 107	0.0082	0.014	0.067
	7	3 - 66	0.012	0.016	0.042
A $^1\Delta$	0	2 - 133	0.0031	0.0058	0.12
	1	3 - 115	0.0045	0.012	0.14
B $^1\Pi_e$	0	1 - 133	0.0043	0.0075	0.065
	1	1 - 116	0.0038	0.011	0.057
	2	1 - 117	0.0048	0.011	0.053
	3	1 - 108	0.0084	0.015	0.062
	4	1 - 116	0.0097	0.02	0.21
	5	2 - 67	0.01	0.018	0.045
B $^1\Pi_f$	0	1 - 133	0.0046	0.0089	0.15
	1	1 - 118	0.0053	0.012	0.052
	2	2 - 115	0.0055	0.013	0.076
	3	2 - 106	0.012	0.02	0.08
	4	2 - 107	0.012	0.023	0.14
	5	3 - 66	0.014	0.019	0.042
C $^1\Sigma^+$	0	0 - 121	0.0041	0.02	0.21
F $^1\Delta$	0	17 - 102	0.057	0.063	0.14
	1	35 - 93	0.057	0.064	0.1
a $^3\Delta_1$	0	2 - 150	0.0026	0.0072	0.063
	1	2 - 150	0.007	0.014	0.12
	2	1 - 150	0.0074	0.013	0.084
	3	2 - 150	0.0072	0.013	0.059
	4	3 - 150	0.012	0.021	0.12
	5	2 - 106	0.0089	0.017	0.06
a $^3\Delta_2$	0	2 - 149	0.0023	0.0086	0.057
	1	1 - 148	0.0052	0.014	0.08
	2	1 - 150	0.0072	0.017	0.2
	3	2 - 147	0.0075	0.018	0.17
	4	3 - 150	0.012	0.021	0.15
	5	2 - 136	0.0089	0.016	0.054
a $^3\Delta_3$	0	3 - 144	0.0024	0.013	0.2
	1	3 - 144	0.0069	0.015	0.15
	2	3 - 145	0.0071	0.012	0.04
	3	3 - 135	0.0077	0.012	0.062
	4	3 - 105	0.012	0.017	0.043
	5	3 - 130	0.0082	0.014	0.055
b $^3\Pi_{0e}$	0	7 - 106	0.0035	0.0065	0.023
b $^3\Pi_{0f}$	0	14 - 91	0.0042	0.0064	0.037
b $^3\Pi_{1e}$	0	11 - 100	0.0035	0.0056	0.013
b $^3\Pi_{1f}$	0	20 - 90	0.0036	0.0058	0.012
b $^3\Pi_{2e}$	0	12 - 111	0.0035	0.0051	0.015
b $^3\Pi_{2f}$	0	12 - 111	0.0035	0.0053	0.031
d $^3\Phi_2$	0	2 - 150	0.0081	0.014	0.14
	1	2 - 151	0.0071	0.013	0.22
	2	2 - 151	0.0075	0.013	0.056
	3	3 - 151	0.0069	0.011	0.035
	4	3 - 106	0.0086	0.014	0.041
d $^3\Phi_3$	0	3 - 148	0.01	0.018	0.12
	1	2 - 151	0.0067	0.011	0.046
	2	2 - 147	0.0071	0.015	0.13

Continued on next page

TABLE 5 – continued from previous page

	v	J Range	Uncertainties (cm^{-1})		
			Min	Av	Max
d $^3\Phi_4$	3	2 - 150	0.0063	0.012	0.09
	4	3 - 136	0.0088	0.014	0.029
	0	4 - 144	0.0081	0.016	0.11
	1	4 - 145	0.0072	0.013	0.053
e $^3\Pi_{0e}$	2	4 - 145	0.0072	0.014	0.16
	3	4 - 145	0.0068	0.013	0.12
	4	4 - 131	0.0082	0.012	0.037
	0	15 - 59	0.058	0.07	0.1
e $^3\Pi_{0f}$	0	27 - 59	0.058	0.064	0.15
e $^3\Pi_{1e}$	0	3 - 73	0.0043	0.02	0.1
e $^3\Pi_{1f}$	0	3 - 67	0.0044	0.016	0.13
e $^3\Pi_2$	0	2 - 85	0.0043	0.034	0.1
f $^3\Delta_1$	0	20 - 76	0.071	0.074	0.1
f $^3\Delta_2$	0	20 - 79	0.071	0.075	0.1
f $^3\Delta_3$	0	21 - 81	0.071	0.077	0.1

3. RESULTS AND DISCUSSION

3.1. Spectroscopic Networks

Figure 2 represents the data from Table 1 showing the experimentally-measured transitions connecting different vibronic states. From this diagram, it is clear that there are three bands connecting the singlet and triplet manifold, and some satellite transitions for the triplet sub-manifolds, allowing most energy levels to be connected.

There are three minor free-floating networks connecting the a $^3\Delta(\nu = 6)$ and d $^3\Phi(\nu = 5)$ levels. These could be connected through observing additional vibrational transitions, but this is not essential for producing a good model of the $^{90}\text{Zr}^{16}\text{O}$ electronic states.

3.2. Energy Levels

Table 4 shows an extract of the final empirical energy levels produced by MARVEL for $^{90}\text{Zr}^{16}\text{O}$ in this work. This list of energy levels includes an estimate for the uncertainty in the provided energy of the quantum state, as well as identifying the number of transitions used to determine the energy level; on average 5.3 transitions were used to find each energy level.

Table 5 summarises the 8088 empirical energy levels found in the main spectroscopic network from the MARVEL analysis for $^{90}\text{Zr}^{16}\text{O}$. We see the minimum, average and maximum uncertainty provided for the empirical energies from the MARVEL analysis. The minimum is usually very small, often less than 0.01 cm^{-1} , while the maximum can exceed 0.1 cm^{-1} ; this is probably for higher J states. There is generally coverage to high rotational number J if the spin-vibronic level is known.

These results show that there is good rotationally-resolved empirical understanding of a reasonable number of vibrational states of the X $^1\Sigma^+$, B $^1\Pi$, a $^3\Delta$ and b $^3\Pi$ electronic states (sufficient for a good potential energy curve to be fitted). However, there is much less vibrational information (only one or two levels) for the A $^1\Delta$,

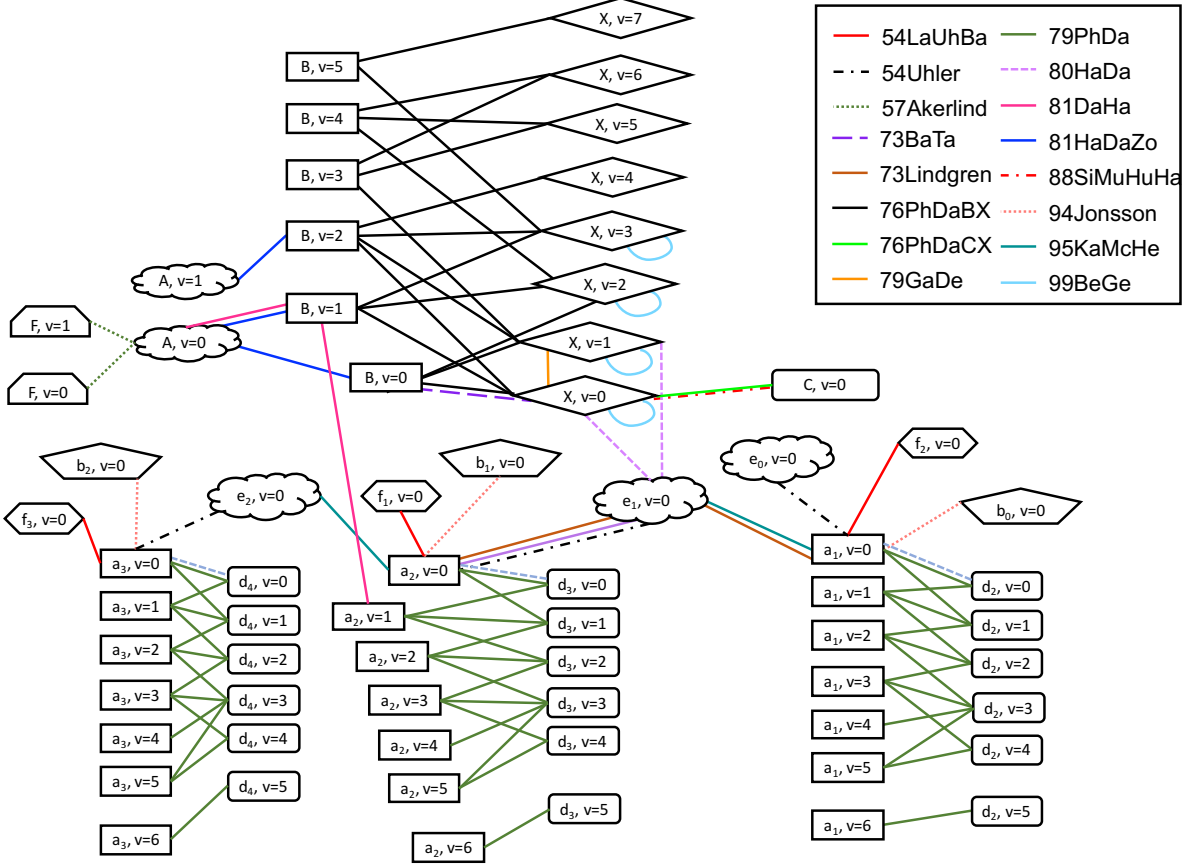


FIG. 2.— Depiction of connectivity of experimentally observed $^{90}\text{Zr}^{16}\text{O}$ bands.

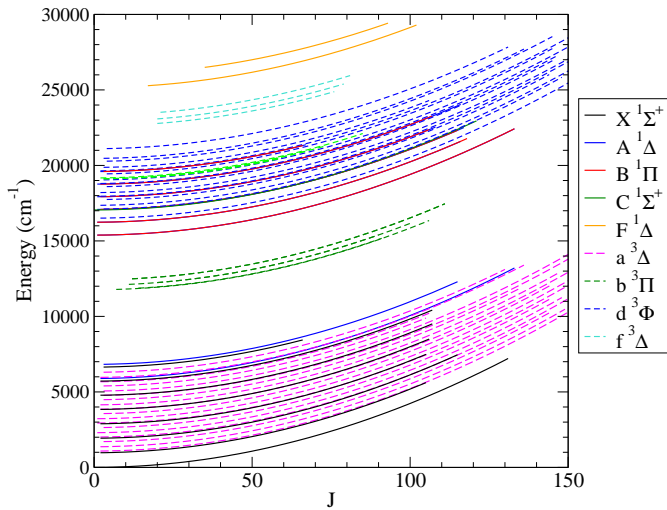


FIG. 3.— $^{90}\text{Zr}^{16}\text{O}$ energy levels from MARVEL analysis.

$\text{C } ^1\Sigma^+$, $\text{F } ^1\Delta$, $\text{b } ^3\Pi$, $\text{e } ^3\Pi$ and $\text{f } ^3\Delta$ states. This will cause significant problems when fitting potential energy curves for a full spectroscopic model and eventual line list for $^{90}\text{Zr}^{16}\text{O}$ and its isotopologues, particularly for the $\text{C } ^1\Sigma^+$, $\text{b } ^3\Pi$, $\text{e } ^3\Pi$, $\text{f } ^3\Delta$ states in which only one vibrational level is known. Note that line lists of all isotopologues can be easily produced using variational nuclear-motion techniques using data from only a single isotopologue with reasonably high accuracy, however *ab initio* predic-

tions of vibrational constants especially for higher lying electronic states of transition-metal-containing diatomics still have errors of up to 50 cm^{-1} (Tennyson et al. 2016).

Figure 3 shows the empirical energy levels for the main spectroscopic network from MARVEL against J for each spin vibronic band. These are clearly quadratic and smooth, indicating there are no major problems with the MARVEL network for $^{90}\text{Zr}^{16}\text{O}$.

3.3. Comparison with Plez et al. (2003)

Figure 4 shows the difference between the singlet MARVEL energy levels for $^{90}\text{Zr}^{16}\text{O}$ and those from the Plez et al. (2003) $^{90}\text{Zr}^{16}\text{O}$ linelist. For the $\text{X } ^1\Sigma^+$, $\text{B } ^1\Pi$ and $\text{C } ^1\Sigma^+$ states, the differences average around $0.05\text{-}0.15 \text{ cm}^{-1}$, with somewhat higher deviations up to 1 cm^{-1} for large J especially in the $\text{C } ^1\Sigma^+$ state. The scatter here is probably largely a reflection of inaccuracies in the MARVEL energy levels, though perturbations not considered in the Plez line list might also contribute. The $\text{A } ^1\Delta$ state, however, shows much more significant deviations; the $v=0$ state is off by about 2 cm^{-1} up to $J=100$, with much more significant deviations for larger J . The $v=1$ state also shows substantial differences of up to 4 cm^{-1} that changes significantly with J .

Figures 5 to 7 shows the difference between the triplet MARVEL energy levels for $^{90}\text{Zr}^{16}\text{O}$ and those from the Plez et al. (2003) $^{90}\text{Zr}^{16}\text{O}$ linelist. These errors are much more significant than for the singlet states.

Clear systematic errors can be seen throughout the $\text{a } ^3\Delta$ and $\text{d } ^3\Phi$ bands - since these are a major cause of

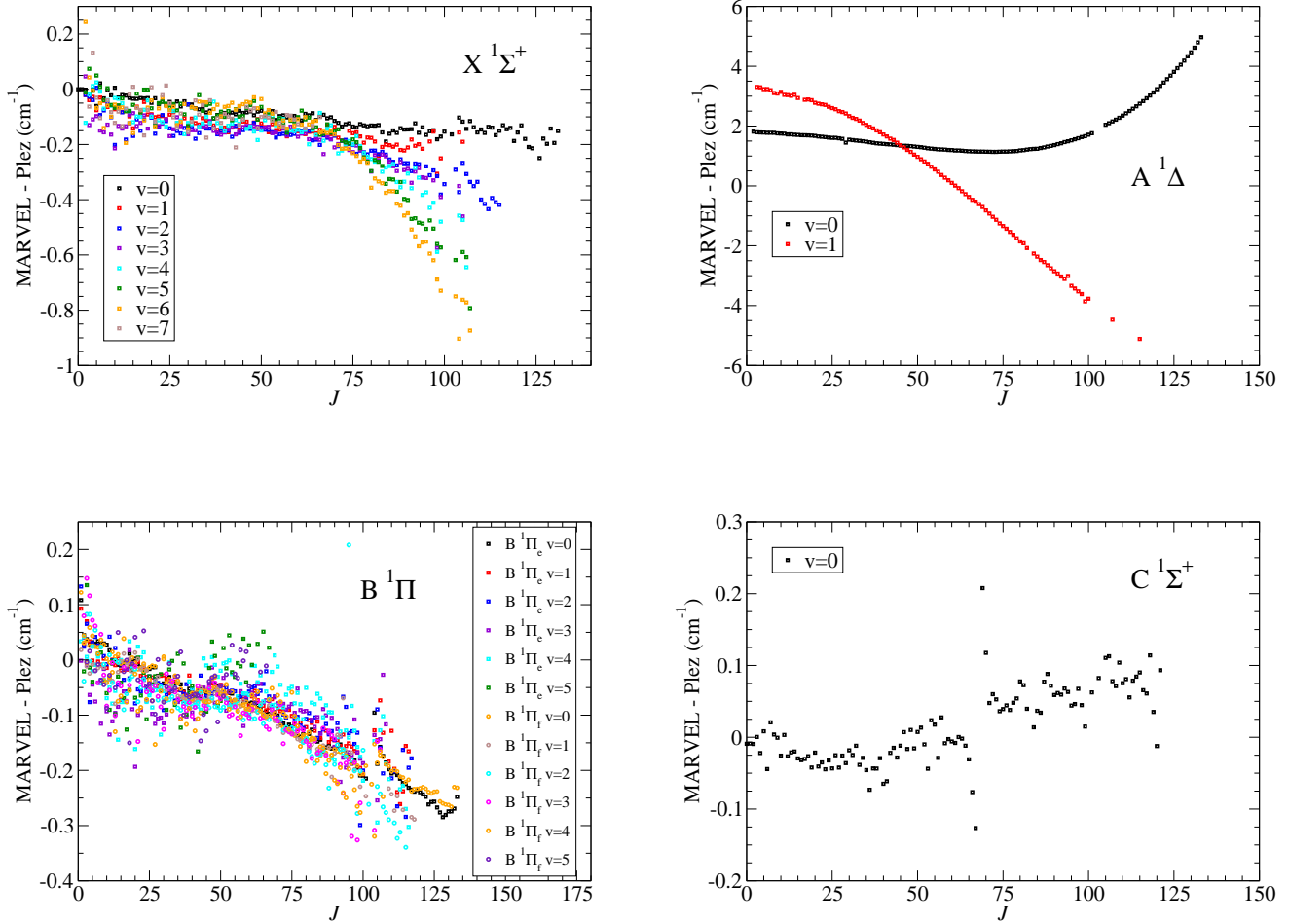


FIG. 4.— Difference between MARVEL and Plez et al. (2003) energy levels for the singlet states.

opacity of $^{90}\text{Zr}^{16}\text{O}$ in stellar conditions, improvements to these energy levels is highly desirable. Note, however, that since the errors in the $a^3\Delta_n$ and $d^3\Phi_{n+1}$ parallel each other, the errors in transition frequencies in the Plez line list will be much smaller than the errors in energies that are plotted here.

The $b^3\Pi$ state shows significant and systematic errors in the Plez database compared to the MARVEL data of up to 15 cm^{-1} for many electronic states. Our adoption of the Jonsson (1994) assignments in preference to the Phillips et al. (1979) assignments contributes to much larger lambda doubling in the MARVEL data than was adopted in the Plez data. There is also clear systematic differences in the energies of the $b^3\Pi_1$ levels of more than 15 cm^{-1} in many regions. Smaller differences of up to 5 cm^{-1} were found in the $b^3\Pi_2$ levels that parallel the errors in the $a^3\Delta_3$ and $d^3\Phi_4$ energies, indicating that the errors associated with the transition frequencies in this band in the Plez line list will be much smaller.

The $f^3\Delta$ data show that Plez's triplet splitting is in error by about 1 cm^{-1} , with some larger errors at high J .

3.4. Band Constants

TABLE 6
SPECTROSCOPIC BAND CONSTANTS, IN cm^{-1} , FOR THE SINGLET VIBRONIC BANDS, ASSUMING NO PERTURBATIONS.

State	v	T_v	B_v	$10^7 D_v$	
$X^1\Sigma^+$	0	-0.028	0.4226	3.18	
	1	969.509	0.42065	3.19	
	2	1932.154	0.41868	3.18	
	3	2887.873	0.41674	3.22	
	4	3836.760	0.41475	3.22	
	5	4778.739	0.41275	3.21	
$A^1\Delta$	0	5887.160	0.41646	3.26	
	1	6823.105	0.41457	3.26	
	$B^1\Pi$	0	15383.385	0.40151	3.51
		1	16236.949	0.39959	3.50
		2	17084.607	0.39765	3.51
		3	17926.299	0.39570	3.51
4		18762.010	0.39375	3.52	
5		19591.668	0.39175	3.40	
$C^1\Sigma^+$	0	17050.378	0.40480	3.44	
$F^1\Delta$	0	25159.631	0.39736	3.57	
	1	25994.872	0.39540	3.66	

TABLE 7
SPECTROSCOPIC CONSTANTS, IN cm^{-1} , FOR THE TRIPLET SPIN-VIBRONIC BAND, ASSUMING NO PERTURBATIONS.

v	$\Sigma = -1$			$\Sigma = 0$			$\Sigma = 1$			$\Delta(SO)$
	T_v	B_v	$D_v(10^7)$	T_v	B_v	$D_v(10^7)$	T_v	B_v	$D_v(10^7)$	
	a $^3\Delta_1$			a $^3\Delta_2$			a $^3\Delta_3$			
0	1080.363	0.41333	3.18	1367.750	0.41476	3.26	1703.505	0.41565	3.43	
1	2011.656	0.41144	3.19	2299.369	0.41285	3.26	2635.505	0.41374	3.44	
2	2936.474	0.40955	3.20	3224.476	0.41096	3.29	3561.029	0.41181	3.45	
3	3854.766	0.40765	3.21	4143.140	0.40903	3.28	4480.011	0.40989	3.45	
4	4766.602	0.40574	3.22	5055.317	0.40712	3.31	5392.650	0.40791	3.43	
5	5672.050	0.40378	3.19	5960.981	0.40516	3.28	6298.588	0.40602	3.48	
	b $^3\Pi_0$			b $^3\Pi_1$			b $^3\Pi_2$			
0	<i>e</i> 11765.173	0.40801	3.36	12069.846	0.40862	3.42	12427.697	0.40934	3.62	
	<i>f</i> 11783.845	0.40754	3.29	12069.859	0.40915	3.45	12427.705	0.40933	3.60	
	d $^3\Phi_2$			d $^3\Phi_3$			d $^3\Phi_4$			
0	16507.187	0.40312	3.57	17109.068	0.40368	3.60	17737.310	0.40430	3.77	
1	17357.358	0.40103	3.58	17958.303	0.40160	3.62	18588.627	0.40222	3.77	
2	18200.953	0.39894	3.59	18801.000	0.39949	3.63	19433.859	0.40015	3.78	
3	19038.014	0.39683	3.60	19637.131	0.39738	3.65	20273.306	0.39807	3.77	
4	19868.503	0.39469	3.58	20466.627	0.39524	3.62	21106.945	0.39602	3.77	
	e $^3\Pi_0$			e $^3\Pi_1$			e $^3\Pi_2$			
0	<i>e</i> 19074.117	0.39551	0.85	19113.069	0.40387	5.73	19169.508	0.40619	5.02	
	<i>f</i> 19078.935	0.39449	0.04	19112.826	0.40266	4.79				
	f $^3\Delta_1$			f $^3\Delta_2$			f $^3\Delta_3$			
0	22616.840	0.38945	3.43	22916.797	0.39207	0.67	23335.153	0.39572	3.01	

Band constants were obtained by a quadratic fit of the energies of the lines against rotational quantum number J for each band.

Table 6 shows the rotational band constants, T_v , B_v and D_v for each singlet vibronic bands. The centrifugal term, D_v is reasonably constant within a given electronic state, while the rotational constants, B_v decreases as expected as the bond length increases in higher vibrational states.

Table 7 shows the fitted rotational band constants for each spin-vibronic band in the triplet manifold for $^{90}\text{Zr}^{16}\text{O}$ from this MARVEL analysis.

A compilation of band constants is given by Kaledin et al. (1995); we find significant differences of 2 cm^{-1} in the T_0 for d $^3\Phi_2$, d $^3\Phi_3$ and a $^3\Delta_3$. We prefer our value, however, as the d $^3\Phi$ -a $^3\Delta$ transitions form part of our input data, whereas it is unclear how the Kaledin et al. (1995) was compiled. Otherwise, the T_0 values agree within 0.1 cm^{-1} .

3.5. Bandheads

Tables 8 to 12 show bandheads predicted by the MARVEL energy levels, compared with available, low-resolution bandhead observations (note that the high resolution bandhead observations are included in the MARVEL input data set). For the singlet states, there is actually only a small number of data points in the B $^1\Pi$ -A $^1\Delta$ band that allow for direct comparison of MARVEL predictions against low-resolution bandhead studies. There are no assigned low-resolution data readily available for the B $^1\Pi$ -X $^1\Sigma^+$ band, and the low-resolution bandhead data for C $^1\Sigma^+$ -X $^1\Sigma^+$ does not overlap with our MARVEL predictions. For the triplets, there is good low-resolution bandhead data for the d $^3\Phi$ -a $^3\Delta$, b $^3\Pi$ -a $^3\Delta$

and e $^3\Pi$ -a $^3\Delta$ bands against which the MARVEL results can be compared; in these cases, there is good agreement for all bands, generally less than 0.5 cm^{-1} (though up to 1.5 cm^{-1}).

The MARVEL results provide predictions for 48 vibronic bands previously unmeasured in low or high resolution spectra. In contrast, there are at least further 68 low resolution bandheads whose position cannot be predicted by our MARVEL data due to lack of information on, usually, the excited state. The most significant missed opportunity for rotational resolved data is in the 48 non-satellite, i.e. $\Delta\Sigma = 0$, e $^3\Pi$ -a $^3\Delta$ bandheads for $v=0$ to $v=6$ observed in low-resolution by Stepanov et al. (1988); note that these data are not reported in this paper. Much lower resolution bandheads are identified by Balfour & Chowdhury (2010) for the C $^1\Sigma^+$ -X $^1\Sigma^+$ band involving excited vibrational levels of the C $^1\Sigma^+$ state; this too warrants further investigation to allow characterisation of the C $^1\Sigma^+$ state.

There have also been some bandheads discussed in previous $^{90}\text{Zr}^{16}\text{O}$ spectroscopic studies which our data unfortunately cannot help assign. Specifically, we don't find any recommended assignment of the double bandhead at 12082.65 cm^{-1} (R head) and 12069.9 cm^{-1} (Q head) observed by Davis & Hammer (1981).

3.6. Equilibrium Constants: Updated recommendations

Table 13 shows equilibrium term energy, vibrational and rotational constants for the X $^1\Sigma^+$, A $^1\Delta$, B $^1\Pi$, F $^1\Delta$, a $^3\Delta_1$, a $^3\Delta_2$, a $^3\Delta_3$, d $^3\Phi_2$, d $^3\Phi_3$, d $^3\Phi_4$ electronic states based entirely on MARVEL energy levels. These equilibrium constants are obtained by fitting to the relevant band constants, with obvious outliers removed for averaging of D_v 's to obtain D . Note that we have chosen

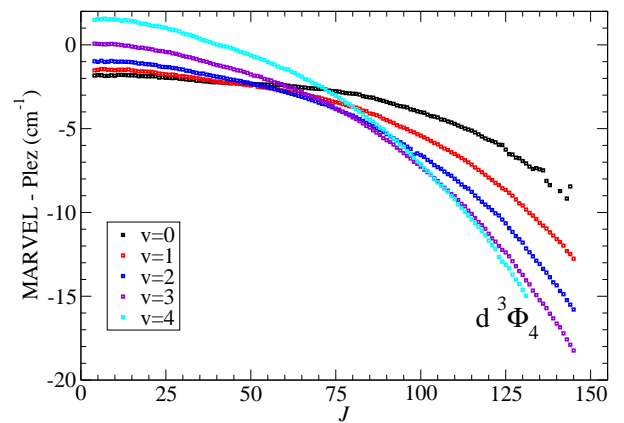
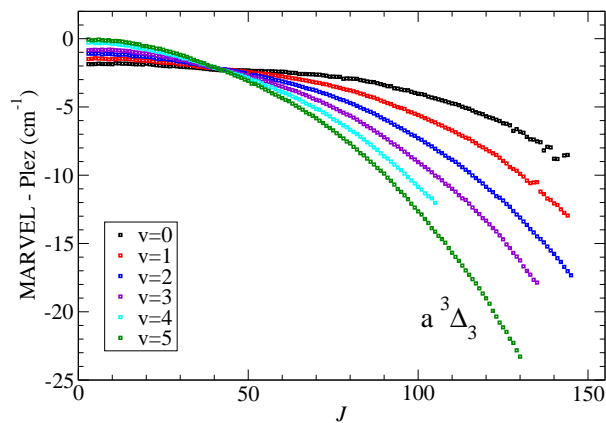
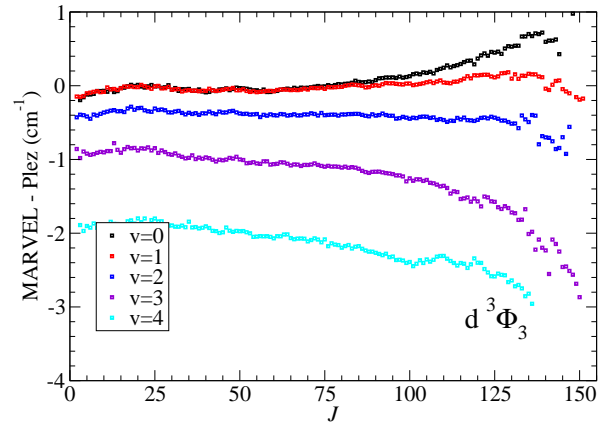
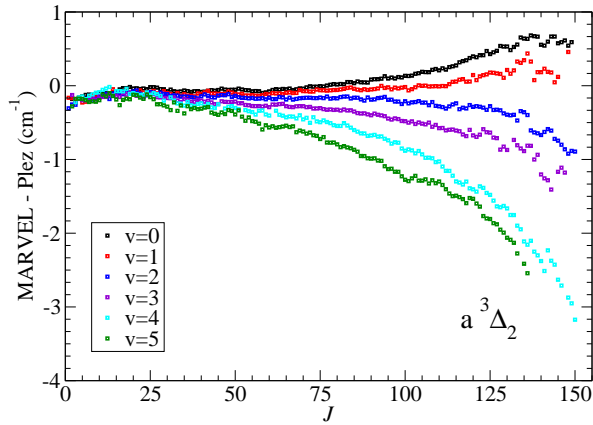
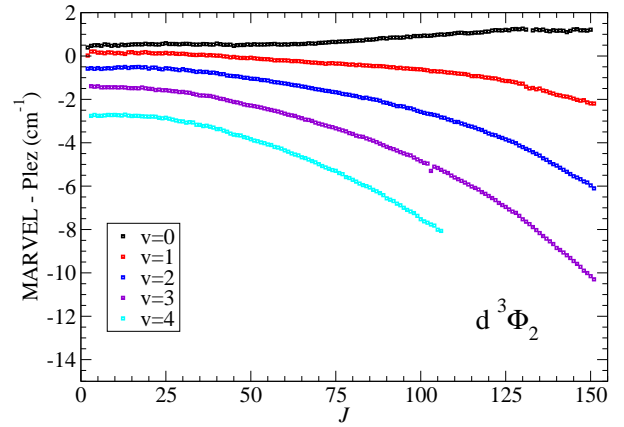
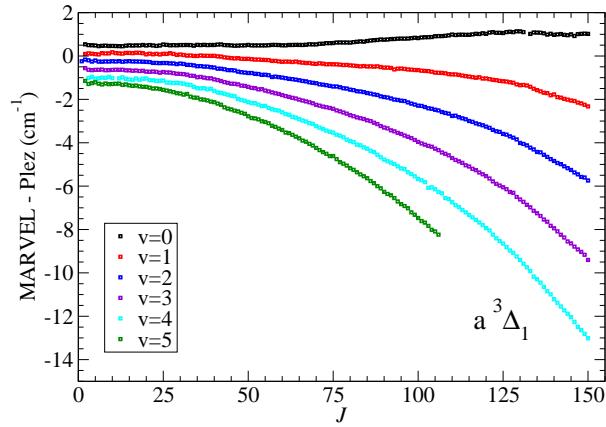


FIG. 5.— Difference between MARVEL and Plez et al. (2003) energy levels for the $a^3\Delta$ state.

FIG. 6.— Difference between MARVEL and Plez et al. (2003) energy levels for the $d^3\Phi$ state.

TABLE 8
R-BRANCH BANDHEADS IN cm^{-1} FROM THE $X^1\Sigma^+$ STATE FOR $^{90}\text{Zr}^{16}\text{O}$; J GIVES THE APPROXIMATE J VALUE CORRESPONDING TO THE ROTATIONAL TRANSITIONS AT THE BANDHEAD.

	$v'-v''$	J	MARVEL	Low-res obs.
$B^1\Pi - X^1\Sigma^+$	0-0	18	15391.40	
	0-1	20	14422.64	
	0-2	22	13460.94	
	0-3*	25	12506.31	
	0-4*	29	11559.08	
	0-5*	34	10619.12	
	0-6*	41	9687.00	
	0-7*	53	8763.33	
	1-0	18	16244.28	
	1-1*	18	15275.39	
	1-2	21	14313.52	
	1-3	22	13358.69	
	1-4*	24	12410.99	
	1-5*	30	11470.63	
	1-6*	36	10537.59	
	1-7*	43	9612.56	
	2-0	15	17091.34	
	2-1	17	16122.32	
	2-2*	18	15160.33	
	2-3	21	14205.29	
	2-4	22	13257.41	
	2-5*	26	12316.62	
	2-6*	30	11383.20	
	2-7*	25	10457.20	
	3-0*	15	17932.50	
	3-1	14	16963.46	
	3-2*	17	16001.36	
	3-3*	17	15046.20	
	3-4*	21	14098.05	
	3-5	22	13157.07	
	3-6	27	12223.20	
	3-7*	31	11296.67	
	4-0*	14	18767.79	
	4-1*	14	17798.67	
	4-2	16	16836.45	
	4-3*	17	15881.27	
	4-4*	17	14933.00	
	4-5	20	13991.83	
	4-6	21	13057.77	
	4-7*	26	12130.78	
	5-0*	11	19597.03	
5-1*	13	18627.83		
5-2*	13	17665.63		
5-3	14	16710.22		
5-4*	17	15761.90		
5-5*	20	14820.57		
5-6*	20	13886.36		
5-7	21	12959.14		
$C^1\Sigma^+ - X^1\Sigma^+$	0-0	22	17059.99	
	0-1*	25	16091.58	
	0-2*	28	15130.40	
	0-3*	33	14176.55	
	0-4*	41	13230.35	
	0-5*	49	12292.37	
	0-6*	82	11365.35	
	1-0			17933 [1]
	2-0			18799 [1]
	3-0			19664 [1]

[1] Balfour & Chowdhury (2010)(converted from wavelength assuming vacuum)

* Bands unobserved in rotationally resolved spectra which have been predicted by MARVEL

TABLE 9
OTHER SINGLET R-BRANCH BANDHEADS IN cm^{-1} FOR $^{90}\text{Zr}^{16}\text{O}$; J GIVES THE APPROXIMATE J VALUE CORRESPONDING TO THE ROTATIONAL TRANSITIONS AT THE BANDHEAD.

	$v'-v''$	J	MARVEL	Low-res obs.	
$F^1\Delta - X^1\Sigma^+$	0-0	17	25166.23		
	0-1	18	24197.07		
	0-2	17	23235.27		
	0-3	22	22280.33		
	0-4	22	21332.47		
	0-5	25	20391.58		
	0-6	30	19458.10		
	0-7	35	18531.99		
	$X^1\Sigma^+ - X^1\Sigma^+$	2-0	101	1975.73	
		3-0	68	2917.35	
		3-1	99	1961.43	
		4-0	51	3858.92	
		4-1	65	2896.33	
		4-2	99	1948.15	
5-0		42	4796.37		
5-1		51	3831.03		
5-2		67	2875.26		
5-3		98	1932.88		
6-0		33	5728.41		
6-1		41	4761.69		
6-2		49	3803.14		
$B^1\Pi - A^1\Delta$	0-0	26	9507.28	9507.45 [1]	
	0-1	30	8572.87		
	1-0	23	10359.55	10359.62 [1]	
	1-1*	25	9424.77	9424.93 [1]	
	2-0	21	11206.15		
	2-1	22	10271.14	10271.26 [1]	
	3-0*	17	12047.00		
	3-1	21	11111.79		
	4-0*	17	12882.08		
	4-1*	17	11946.74		
	5-0*	15	13711.04		
	5-1*	17	12775.64		
	$C^1\Sigma^+ - A^1\Delta$	0-0*	33	11177.59	
0-1*		41	10244.31		
$F^1\Delta - A^1\Delta$	0-0	22	19281.19		
	0-1	22	18346.21		

[1] Balfour & Chowdhury (2010)(converted from wavelength assuming vacuum)

* Bands unobserved in rotationally resolved spectra which have been predicted by MARVEL

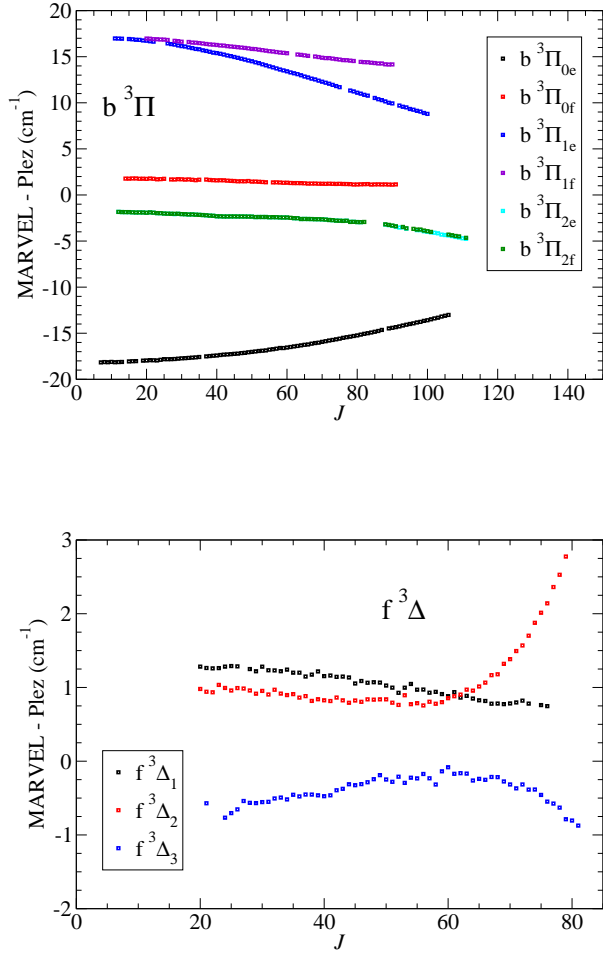


FIG. 7.— Difference between MARVEL and Plez et al. (2003) energy levels for the $b^3\Pi$ and $f^3\Delta$ state.

TABLE 10
OTHER SINGLET R-BRANCH BANDHEADS IN cm^{-1} FOR $^{90}\text{Zr}^{16}\text{O}$; J
GIVES THE APPROXIMATE J VALUE CORRESPONDING TO THE
ROTATIONAL TRANSITIONS AT THE BANDHEAD.

	$v'-v''$	J	MARVEL
$F^1\Delta - B^1\Pi$	0-0	91	9814.07
	1-0	61	10637.34
	1-1	90	9794.47
$B^1\Pi - C^1\Sigma^+$	2-0	53	56.81
	3-0	41	893.65
	4-0	34	1726.14
	5-0	28	2553.57
$F^1\Delta - C^1\Sigma^+$	0-0	50	8130.59
	1-0	40	8961.46

TABLE 11
TRIPLET $b^3\Pi - a^3\Delta$, AND $e^3\Pi - a^3\Delta$ R-BRANCH BANDHEADS IN
 cm^{-1} FOR $^{90}\text{Zr}^{16}\text{O}$; J GIVES THE APPROXIMATE J VALUE
CORRESPONDING TO THE ROTATIONAL TRANSITIONS AT THE
BANDHEAD.

	$v'-v''$	J	MARVEL	Low-res obs.
$e^3\Pi_1 - X^1\Sigma^+$	0-0			19124 [1]
	1-0			19963 [1]
	2-0			20784 [1]
$b^3\Pi_{0e} - a^3\Delta_1$	0-0	72	10715.52	10715.26 [3]
	0-1*	101	9798.16	
	1-1			10634.15 [3]
$b^3\Pi_{0f} - a^3\Delta_1$	0-0	67	10731.97	10731.92 [1]
$b^3\Pi_{1e} - a^3\Delta_2$	0-0	63	10729.02	10728.98 [1]
	0-1*	89	9808.11	
$b^3\Pi_{1f} - a^3\Delta_2$	0-0	67	10731.44	10731.29 [1]
	1-1			10649.82 [3]
$b^3\Pi_2 - a^3\Delta_3$	0-0	62	10750.52	
	0-1	81	9828.65	
$e^3\Pi_{1e} - a^3\Delta_2$	0-0	34	17760.35	
	0-1*	40	16831.39	16833.0 [2]
	0-2*	49	15909.87	15909.2 [2]
	0-3*	58	14996.56	14994.3 [2]
$e^3\Pi_{1f} - a^3\Delta_2$	0-0	32	17758.67	
	0-1*	38	16829.39	16833.0 [2]
	0-2*	44	15907.41	15909.2 [2]
	0-3*	55	14993.55	14994.5 [2]
$e^3\Pi_1 - a^3\Delta_2$	1-1			17669.2 [2]
	1-2			16747.2 [2]
	1-3			15556.1 [2]
	1-4			14923.9 [2]

[1] Measured (Davis & Hammer 1981) reassigned here, [2] Stepanov et al. (1988), [3] Balfour & Chowdhury (2010) (converted from wavelength assuming vacuum)

* Bands unobserved in rotationally resolved spectra which have been predicted by MARVEL

to provide constants for the various sub-components of the triplet levels individually rather than use additional constants to unify their treatment.

Based on a comprehensive collation and critical analysis of all available information (to our knowledge) of spectroscopic constants, we can go beyond this MARVEL analysis to provide recommendations for all equilibrium constants for the electronic states of $^{90}\text{Zr}^{16}\text{O}$; these are shown in Table 14 and Table 15. Some of these constants come solely from the MARVEL analysis in this paper, but some use other sources of data, particularly for vibrational anharmonicities where lower resolution bandhead data can provide additional information. Note that because we do not consider higher order corrections to D or α within these constants, we use D and α rather than D_e and α_e .

Note that these constants will provide less accurate information on particular energy levels than the raw MARVEL energy levels, but have the advantages of being a smaller, more easily parsed set of numbers. Thus, we have chosen to average across different parity and spin states in most cases, though we retain the term values (T_e) for individual spin components of the triplet states.

The justification for each of the constants in Table 14 and Table 15 are as follows:

- $X^1\Sigma^+$: The MARVEL values were chosen for the main spectroscopic constants, with rounding and

TABLE 12
 $d^3\Phi$ - $a^3\Delta$ R-BRANCH BANDHEADS IN cm^{-1} FOR $^{90}\text{Zr}^{16}\text{O}$ FROM THE MAIN SPECTROSCOPIC NETWORKS; J GIVES THE LOCATION OF THE BANDHEAD IN OUR DATA.

v^1-v^0	J	MARVEL	Low-res obs.	J	MARVEL	Low-res obs.	J	MARVEL	Low-res obs.
		$d^3\Phi_2 - a^3\Delta_1$		$d^3\Phi_3 - a^3\Delta_2$		$d^3\Phi_4 - a^3\Delta_3$			
0-0	39	15443	15443.0 [1]	34	15756.3	15756.3 [1]	36	16048.46	16048.6 [1]
0-1	48	14515.12		43	14827.63		42	15119.3	15119.2 [1]
0-2*	57	13595.58		52	13906.89		51	14198.01	
0-3*	78	12686.13		67	12995.36		68	13285.67	
0-4*	108	11790.97		96	12096.25		90	12385.29	
1-0	32	16290.36	16290.4 [1]	30	16603.14	16603.4 [1]	30	16897.5	16897.4 [1]
1-1	37	15361.4	15361.4 [1]	34	15673.57	15673.5 [1]	35	15967.47	15967.9 [1]
1-2	44	14439.86		40	14751.22		40	15044.66	15044.0 [1]
1-3*	57	12526.53		51	13836.77		51	14129.7	
1-4*	76	12623.07		68	12931.37		67	13223.55	
1-5*	104	11733.3		94	12047.9		87	12329	
2-0*	27	17132.02	17132.9 [1]	26	17444.03	17444.7 [1]	25	17741.09	
2-1			16202.5 [1]	28	16513.89	16514.0 [1]	29	16810.47	16810.6 [1]
2-2	36	15279.76	15279.8 [1]	34	15590.72	15590.8 [1]	33	15886.85	15886.9 [1]
2-3*	45	14364.58		40	14674.79		39	14970.55	14970.7 [1]
2-4*	54	13457.5		51	13766.6		51	14061.86	
2-5*	74	12560.01		64	12867.46		64	13161.97	
3-0*	23	17967.59		22	18278.87		23	18579.17	
3-1*	26	17037.47	17036.2 [1]	24	17348.38	17347.7 [1]	25	17648.31	17646.7 [1]
3-2	29	16114.24	16114.2 [1]	27	16424.59	16424.7 [1]	29	16724.12	16724.3 [1]
3-3	35	15198.07	15298.4 [1]	34	15507.83	15508.2 [1]	33	15807.01	15807.6 [1]
3-4	41	14289.18		39	14597.25		40	14897.02	14897.2 [1]
3-5	54	13388.34		47	13696.37		51	13994.73	
4-0*	21	18796.88		19	19107.25		19	19411.79	
4-1*	24	17866.54		21	18176.52		22	18480.69	
4-2*	25	16942.87	16942.5 [1]	24	17252.48	17253.3 [1]	24	17556.27	17555.6 [1]
4-3	29	16026.05	16025.0 [1]	28	16335.14	16335.6 [1]	27	16638.61	16638.6 [1]
4-4*	36	15116.29	15115.2 [1]	34	15424.86	15425.2 [1]	31	15727.82	15728.3 [1]
4-5	43	14213.74		39	14521.64		39	14824.26	
5-3*			16847.4 [1]						17463.2 [1]
5-4*			15936.9 [1]						16554.2 [1]
5-5*			15034.8 [1]			15342.6 [1]			15648.8 [1]

[1] Stepanov et al. (1988)

* Bands unobserved in rotationally resolved spectra which have been predicted by MARVEL

TABLE 13
EQUILIBRIUM VIBRATIONAL CONSTANTS, IN cm^{-1} , BASED SOLELY ON MARVEL ENERGY LEVELS.

State	T_e	ω_e	$\omega_e\chi_e$	B_e	$\alpha(10^3)$	$D(10^7)$
X $^1\Sigma^+$	0	976.44	3.45	0.42361	1.97	3.19
A $^1\Delta$	5906.58	935.95	-	0.41741	1.89	3.26
B $^1\Pi$	15441.70	859.59	2.99	0.40246	1.90	3.50
F $^1\Delta$	25229.40	835.24	-	0.39834	1.96	3.60
a $^3\Delta_1$	1099.70	937.74	3.23	0.41430	1.91	3.19
a $^3\Delta_2$	1386.90	938.09	3.24	0.41573	1.92	3.26
a $^3\Delta_3$	1722.45	938.51	3.25	0.41663	1.93	3.43
d $^3\Phi_2$	16567.04	856.72	3.27	0.40419	2.11	3.57
d $^3\Phi_3$	17169.35	855.84	3.29	0.40475	2.11	3.61
d $^3\Phi_4$	17796.92	857.09	2.94	0.40533	2.07	3.77

TABLE 14
RECOMMENDED UPDATED EQUILIBRIUM CONSTANTS IN cm^{-1} FOR TRIPLET STATES OF $^{90}\text{Zr}^{16}\text{O}$, WITH BOND LENGTHS IN \AA . THE VALUE IN THE PARENTHESIS IS THE UNCERTAINTY IN THE LAST FIGURE. JUSTIFICATIONS FOR EACH ELECTRONIC STATE ARE PROVIDED IN THE TEXT.

State	T_e	ω_e	$\omega_e x_e$	B_e	$\alpha(10^{-3})$	$D(10^{-7})$	r_e
X $^1\Sigma^+$	0.0	976.44(2)	3.44(2)	0.4236(1)	1.97(2)	3.2(1)	1.712(2)
A $^1\Delta$	5906.6(2)	942.3(2)	3.1(1)	0.4174(1)	1.89(1)	3.3(1)	1.725(2)
B $^1\Pi$	15441.7(2)	859.6(2)	3.0(1)	0.4025(1)	1.90(1)	3.5(2)	1.756(2)
C $^1\Sigma^+$	17101(1)	876(1)	3.0(2)	0.4056(1)	1.65(1)	3.4(1)	1.750(3)
F $^1\Delta$	25227(1)	841(1)	2.9(2)	0.3983(3)	2.0(1)	3.6(2)	1.765(2)

TABLE 15
 RECOMMENDED UPDATED EQUILIBRIUM CONSTANTS IN cm^{-1} FOR SINGLET STATES OF $^{90}\text{Zr}^{16}\text{O}$, WITH BOND LENGTHS IN \AA . SQUARE BRACKETS INDICATE THE DATA IS ONLY FROM $v=0$. THE VALUE IN THE PARENTHESIS IS THE UNCERTAINTY IN THE LAST FIGURE. JUSTIFICATIONS FOR EACH ELECTRONIC STATE ARE PROVIDED IN THE TEXT.

State	T_e $_{ \Omega = \Lambda-1 }$	T_e $_{ \Omega = \Lambda }$	T_e $_{ \Omega = \Lambda+1 }$	ω_e	$\omega_e x_e$	B_e	α_e (10^{-3})	D (10^{-7})	r_e
a $^3\Delta$	1099.7(7)	1386.9(5)	1722.4(9)	938.1(4)	3.24(1)	0.415(1)	1.93(4)	3.3(1)	1.729(2)
b $^3\Pi$	11807(1), 11826(1)	12112(1)	12469(4)	890(1)	3.2(3)	[0.409](1)		3.5(3)	1.741(2)
d $^3\Phi$	16567(1)	17169(1)	17796(1)	855(1)	3.0(2)	0.404(1)	2.10(3)	3.6(1)	1.751(2)
e $^3\Pi$	19138(1), 19142(1)	19177(1)	19233(1)	846(1)	3.1(2)	[0.401](1)		5(2)	1.756(2)
f $^3\Delta$	22692(1)	22993(1)	23411(1)	821(1)	3.3(2)	[0.392](2)		3.1(6)	1.776(2)

uncertainties determined by comparison of MARVEL values from Phillips & Davis (1976b) and, for rotational constants, Beaton & Gerry (1999).

- A $^1\Delta$: Rotational constants are from MARVEL analysis, while the equilibrium vibrational constants are taken from Hammer & Davis (1981) (only values available). Consistency with MARVEL T_v 's has been checked. Note that Hammer & Davis (1981) has rotational band constants and equilibrium vibrational constants involving A $^1\Delta$ $v > 1$, but doesn't provide transition data involving this level thus its exclusion from the MARVEL compilation.
- B $^1\Pi$: Constants from MARVEL analysis, with uncertainties based on differences between MARVEL and Phillips & Davis (1976b)/Hammer & Davis (1981). Contributions from the e and f parity bands were averaged.
- C $^1\Sigma^+$: Vibrational constants are taken from Murty (1980a) which is based on mostly Phillips & Davis (1976a) data. B_e and α_e were also from Murty (1980a) with uncertainties chosen to ensure consistency with other available data, including MARVEL's B_0 values. The centrifugal distortion term D is by necessity a $v=0$ constant rather than an equilibrium value and thus is taken from MARVEL with uncertainties determined by comparison to Simard et al. (1988b) and Phillips & Davis (1976a). Recommended equilibrium term energy T_e is based on T_0 from MARVEL data and the adopted vibrational constants.
- F $^1\Delta$: Based on values for other states, $\omega_e x_e = 2.9(2)$ seems reasonable; we use this value and other MARVEL T_e data to obtain equilibrium term energy and vibrational constants. Rotational constants are taken from MARVEL values.
- a $^3\Delta$: MARVEL data is used, averaged over the various spin states for vibrational and rotational equilibrium constants. Uncertainties are estimated largely based on the difference between constants of the three different spin components.
- b $^3\Pi$: Rotational resolution and thus MARVEL data is only available for the $v=0$ levels; thus rotational $v = 0$ band constants are provided rather than rotational equilibrium constants, while vibrational constants are taken from Jonsson (1994). Uncertainties in rotational band constants were estimated by comparing values from the different spin components. Uncertainties in vibrational constants were taken as 1 cm^{-1} based on typical differences between vibrational constants for the three spin components for ZrO triplet states.
- d $^3\Phi$: Constants are taken from MARVEL data, with uncertainties estimated based on the difference between the constants from the three different spin components.
- e $^3\Pi$: There are no rotationally resolved $v > 0$ data, so we recommend vibrational equilibrium constants

from Stepanov et al. (1988) based on bandhead data. Rotational data is band constants from MARVEL $v=0$ levels. The equilibrium term energies, T_e are calculated from the adopted equilibrium constants and MARVEL T_0 values. Note that there is significant enough Λ -doubling in the $e^3\Pi_0$ levels to justify separate report of different T_e values, whereas this effect is negligible at the likely accuracy of these constants for the $e^3\Pi_1$ and $e^3\Pi_2$ level.

- f $^3\Delta$: The Huber & Herzberg (1979) (HH) data has been retained for the vibrational equilibrium constants since there has been no subsequent experiments involving this state and no rotationally resolved spectral data for levels above $v = 0$ that could be utilised in the MARVEL analysis. For the rotational constants, MARVEL data has been used, with uncertainties determined by the difference between the MARVEL and HH values (these are quite close) and the spread of values amongst different spin components. Note that the fitted D_0 constants for the f $^3\Delta_2$ band seems erroneous and is likely the result of perturbations; thus it has been largely ignored in the averaging. The equilibrium term energies, T_e , are based on MARVEL T_0 and HH vibrational constants.

The spectroscopic constants given in Tables 14 and 15 can be considered to provide a much needed update the $^{90}\text{Zr}^{16}\text{O}$ entry in the still very commonly used Huber & Herzberg (1979) (HH) compilation of diatomic constants. Note that the HH data was collated up to August 1975, i.e. before a substantial number of the experiments, particularly the infrared spectra of Gallaher & Devore (1979) and many spectra recorded by Davis and co-authors over the 1970s and 80s. There have been significant relabelling of the electronic states over the years; we adopt the convention shown in Figure 1, with some other labels, including the HH labels, shown in brackets. Our comments here use the updated notation.

A key difference between HH and our recommendations is in the harmonic vibrational frequency of the X $^1\Sigma^+$ ground state: 969.7 cm^{-1} (HH) vs 976.38 cm^{-1} (MARVEL and our recommended value). This difference arises because the HH value is taken from a neon matrix spectrum (rather than a gas phase spectrum) which is known to cause shifts in vibrational frequencies.

All triplet states and the A $^1\Delta$ state harmonic vibrational frequencies from HH were obtained from bandhead data; we update the A $^1\Delta$, a $^3\Delta$ and b $^3\Pi$ values with rotationally-resolved data. For all states except the X $^1\Sigma^+$, C $^1\Sigma^+$ and b $^3\Pi$ states, the harmonic vibrational constants from Huber & Herzberg (1979) are within $2\text{-}4 \text{ cm}^{-1}$ of our results. Our C $^1\Sigma^+$ and b $^3\Pi$ vibrational constants are based on low-resolution results from Balfour & Chowdhury (2010) and would need to be further verified; however, they should be more reliable than those of HH.

HH does not contain any information on the observed C $^1\Sigma^+$ or b $^3\Pi$ states or the theoretically predicted D $^1\Gamma$, E $^1\Phi$ and c $^3\Sigma^-$ states. HH did not have access to the triplet-singlet separation, instead leaving an 'x' offset between the singlet and triplet manifolds. This was

measured by Hammer & Davis (1980) as 1100 cm^{-1} . The T_e for the B $^1\Pi$, a $^3\Delta$, d $^3\Phi$ and e $^3\Pi$ states are within 2 cm^{-1} (MARVEL vs. HH). HH doesn't have absolute or relative T_e for the A $^1\Delta$ state.

Therefore, the key updates to HH from our results are:

- updated vibrational constants for the X $^1\Sigma^+$ state;
- inclusion of the b $^3\Pi$, C $^1\Sigma^+$ state;
- absolute T_e of the A $^1\Delta$ state;
- absolute T_e for triplet states.

These updates are important to note given the widespread use of the HH constants for a wide variety of applications from benchmarking quantum chemistry (Langhoff & Bauschlicher Jr 1990) to calculating partition functions and equilibrium constants for astrophysical atmosphere models (Sauval & Tatum 1984; Barklem & Collet 2016).

We note that we are not the first, of course, to update some of the HH constants (e.g. see Afaf (1987); Davis & Hammer (1988); Langhoff & Bauschlicher Jr (1990)); this update is, however, comprehensive and based on a complete self-consistent data set containing all available assigned rovibronic spectra of ZrO.

3.7. Partition Function

Table 16 shows the partition function for $^{90}\text{Zr}^{16}\text{O}$ at a range of temperatures. These are predicted in two ways: using just MARVEL energy levels and using MARVEL energy levels and the contributions from rovibronic states not in the MARVEL collation up to $v=15$ and $J=300$ for the X $^1\Sigma^+$, A $^1\Delta$, B $^1\Pi$, C $^1\Sigma^+$, a $^3\Delta$, b $^3\Pi$, d $^3\Phi$ and e $^3\Pi$ states. We also compare against results from Shankar & Littleton (1983), Sauval & Tatum (1984) and Barklem & Collet (2016). From these results, it is obviously essential at high temperatures to incorporate the effect of energy levels not considered in the MARVEL collation of energy levels (i.e. extrapolate beyond available experimental data). When this is done, the four results are all consistent within 2.6 % at 5000 K. The key differences between the methodology for these four results are (1) explicit summation of energy levels as done in this paper vs high temperature summation expression used by previous authors, (2) the number of electronic states considered, and (3) minor changes in the spectroscopic constants used. We have checked the convergence of the explicit sum of our partition function in terms of the values of v and J and the number of electronic states included and found it to be consistent within 4 significant figures, the accuracy of our input constants, at 5000 K. Therefore, we recommend using our MARVEL + constants partition function values, as tabulated at 1 K intervals in the Supporting Information.

3.8. Recommended Experiments

It would be desirable to obtain rovibronically resolved spectra involving the higher vibrational states for the e $^3\Pi$, b $^3\Pi$, and C $^1\Sigma^+$ states (for which only $v=0$ is measured) and the A $^1\Delta$ and F $^1\Delta$ states (for which only $v=0$ and $v=1$ are measured). This is critical for a high quality spectroscopic study of the molecule;

currently, line lists would need to rely on lower quality non-rotationally resolved data to understand the vibrational structure. We can use the theoretical investigation of $^{90}\text{Zr}^{16}\text{O}$ by Langhoff & Bauschlicher Jr (1990) to guide our predictions for the ease of detecting these new transitions. The A $^1\Delta$ state is only reasonably accessible via relaxation or stimulated emission from the B $^1\Pi$ state or through high temperature initial population; several vibrational level of B $^1\Pi$ can be populated through observed, high intensity, transitions, however. The C $^1\Sigma^+$ state is directly accessible from the ground X $^1\Sigma^+$ state; the spectral region for the C $^1\Sigma^+ - X^1\Sigma^+$ 1-0 transition is estimated at around $18,000\text{ cm}^{-1}$ and should have reasonable Franck-Condon intensity. Other vibronic bands of b $^3\Pi - a^3\Delta$ will probably be fairly weak due to near diagonal Franck-Condon factors, lower populations of vibrationally excited a $^3\Delta$ and low b $^3\Pi - a^3\Delta$ dipole moments. However, these bands should be detectable with few spectrally close bands interfering in absorption.

A high resolution infrared spectrum would be desirable; the only study of Gallaher & Devore (1979) has very poor resolution (0.1 cm^{-1}).

4. CONCLUSIONS

We collate all suitable available assigned $^{90}\text{Zr}^{16}\text{O}$ experimental high-resolution spectroscopy data. We use 23 317 assigned transitions to produce 8088 energy levels in a single spectroscopic networks spanning 9 electronic states and 72 total spin-vibronic bands.

The Supplementary Information to this paper contains three main files: 90Zr-16O.marvel.inp which contains the final input data of spectroscopic transitions in MARVEL format, 90Zr-16O.marvel.out which contains the final output energies from multiple spectroscopic networks and 90Zr-16O.energies which contains the sorted energies in the main spectroscopic network.

Much of the data for $^{90}\text{Zr}^{16}\text{O}$ is quite outdated (for example, the F $^1\Delta$ state has not been investigated in more than 60 years) and would benefit from re-measurements with modern high quality techniques; it is likely some additional spin vibronic bands can be identified. However, the most pressing experimental needs for $^{90}\text{Zr}^{16}\text{O}$ are high-resolution studies of:

- the infrared spectra;
- transitions that access higher vibrational levels of the A $^1\Delta$, C $^1\Sigma^+$ and b $^3\Pi$ state;
- the e $^3\Pi - X^1\Sigma^+$ transitions described by Balfour & Chowdhury (2010); this would enable another confirmation of the triplet-singlet energy separation.

These future advances would enable significant improvements to the current understanding of the rovibronic energy-level structure of $^{90}\text{Zr}^{16}\text{O}$. New experimental data can readily be added to the existing MARVEL database for $^{90}\text{Zr}^{16}\text{O}$ to produce updated empirical energy levels. These studies would substantially improve the quality of line lists for $^{90}\text{Zr}^{16}\text{O}$.

Finally we note that a major part of this work was performed by 16 and 17 year old pupils from the Highams Park School in London, as part of a project known

TABLE 16
PARTITION FUNCTION FOR $^{90}\text{Zr}^{16}\text{O}$ AS A FUNCTION OF TEMPERATURE(T) ESTIMATED BASED ON THE NEW MARVEL DATA AND REASONABLE
EXTRAPOLATIONS.

T / K	0	1	10	100	300	500	800	1000	1500	2000	3000	5000
MARVEL only	1.	2.02446	16.8071	164.881	506.325	1006.32	2508.94	4185.61	11082.6	21884.9	53261.5	136797.
MARVEL + constants	1.	2.02446	16.8071	164.881	506.398	1006.87	2510.93	4190.11	11157.3	22472.4	59845.3	209393.
Shankar & Littleton (1983)								4184.00	11140.0	22450.0	59790.0	211700.
Sauval & Tatum (1984)								4167.99	11333.9	22729.5	60236.7	208621.
Barklem & Collet (2016)	1	2.02843	16.8283	165.280	507.801	1010.06		4209.23	11234.5	22679.4	60617.8	214087.

as ORBYTs (Original Research By Young Twinkle Students). Three other Marvel studies were undertaken in 2016 as part of the ORBYTS project, on $^{48}\text{Ti}^{16}\text{O}$ (McKemmish et al. 2017) and the parent isotopologues of methane (Barton et al. 2018) and acetylene (Chubb et al. 2018b). Another study on H_2S (Chubb et al. 2018a) was performed concurrently with this study in the 2016-17 academic year. Sousa-Silva et al. (2018) discusses our experiences of working with school students to perform high-level research.

ACKNOWLEDGMENTS

We would like to thank Jon Barker, Fawad Sheikh and Highams Park School for support and helpful discussions.

We thank Bob Kurucz for providing data very quickly.

This project has been supported by funding from the European Union Horizon 2020 research and innovation programme under the Marie Skłodowska-Curie grant agreement No 701962, and by UK Science and Technology Research Council(STFC) No. ST/M001334/1.

The work performed in Hungary was supported by the NKFIH(grant no. K119658). The collaboration between the London and Budapest teams received support from COST action CM1405, MOLIM: Molecules in Motion.

REFERENCES

- Afaf, M. 1949, *Nature*, 164, 752
—, 1950a, *Proc. Phys. Soc. A*, 63, 1156
—, 1950b, *Proc. Phys. Soc. A*, 63, 674
—, 1987, *ApJ*, 314, 415
—, 1995, *ApJ*, 447, 980
Ake, T. B. 1979, *ApJ*, 234, 538
Åkerlind, L. 1956, *Naturwissenschaften*, 43, 103
Åkerlind, L. 1957, *Arkiv for Fysik*, 11, 395
Al Derzi, A. R., Furtenbacher, T., Yurchenko, S. N., Tennyson, J., & Császár, A. G. 2015, *J. Quant. Spectrosc. Radiat. Transf.*, 161, 117
Árendás, P., Furtenbacher, T., & Császár, A. G. 2016, *J. Math. Chem.*, 54, 806
Balfour, W. J., & Chowdhury, P. K. 2010, *Chem. Phys. Lett.*, 485, 8
Balfour, W. J., & Lindgren, B. 1980, *Physica Scripta*, 22, 36
Balfour, W. J., & Tatum, J. B. 1973, *J. Mol. Spectrosc.*, 48, 313
Barklem, P. S., & Collet, R. 2016, *A&A*, 588, A96
Barton, E. J., Liu, M., T., F., Tennyson, J., & Sousa-Silva, C. 2018, *JQSRT* (to be submitted)
Beaton, S. A., & Gerry, M. C. 1999, *J. Chem. Phys.*, 110, 10715
Bijc, B., Cmiphov, A. D., Cyclov, A. A., et al. 1974, *J. Quant. Spectrosc. Radiat. Transf.*, 14, 221
Bobrovnikoff, N. T. 1934, *ApJ*, 79, 483
Brown, J. M., Hougén, J. T., Huber, K. P., et al. 1975, *J. Mol. Spectrosc.*, 55, 500
Chubb, K. L., Naumenko, O. V., Keely, S., et al. 2018a, *J. Quant. Spectrosc. Radiat. Transf.*, (submitted)
Chubb, K. L., Joseph, M., Franklin, J., et al. 2018b, *J. Quant. Spectrosc. Radiat. Transf.*, 204, 42
Császár, A. G., Czakó, G., Furtenbacher, T., & Mátyus, E. 2007, *Annu. Rep. Comput. Chem.*, 3, 155
Császár, A. G., & Furtenbacher, T. 2011, *J. Mol. Spectrosc.*, 266, 99
Davis, S. P., & Hammer, P. D. 1981, *ApJ*, 250, 805
—, 1988, *ApJ*, 332, 1090
Furtenbacher, T., Árendás, P., Mellau, G., & Császár, A. G. 2014, *Sci. Rep.*, 4, 4654
Furtenbacher, T., Coles, P. A., Tennyson, J., & Császár, A. G. 2018, *J. Quant. Spectrosc. Radiat. Transf.*, To be submitted
Furtenbacher, T., & Császár, A. G. 2012a, *J. Quant. Spectrosc. Radiat. Transf.*, 113, 929
—, 2012b, *J. Molec. Struct. (THEOCHEM)*, 1009, 123
Furtenbacher, T., & Császár, A. G. 2018, *MARVEL* online, <http://kkrk.chem.elte.hu/marvelonline>
Furtenbacher, T., Császár, A. G., & Tennyson, J. 2007, *J. Mol. Spectrosc.*, 245, 115
Furtenbacher, T., Szabó, I., Császár, A. G., et al. 2016, *ApJS*, 224, 44
- Furtenbacher, T., Szidarovszky, T., Fábri, C., & Császár, A. G. 2013a, *Phys. Chem. Chem. Phys.*, 15, 10181
Furtenbacher, T., Szidarovszky, T., Mátyus, E., Fábri, C., & Császár, A. G. 2013b, *J. Chem. Theo. Comp.*, 9, 5471
Gallaher, T. N., & Devore, T. C. 1979, *High Temp. Sci.*, 11, 123
Green, D. 1969, *High Temp. Sci.*, 1, 26
Hammer, P. 1978, *PASP*, 90, 491
Hammer, P. D., & Davis, S. P. 1979, *J. Mol. Spectrosc.*, 78, 337
Hammer, P. D., & Davis, S. P. 1980, *ApJL*, 237, L51
Hammer, P. D., & Davis, S. P. 1981, *ApJS*, 47, 201
Hammer, P. D., Davis, S. P., & Zook, A. C. 1981, *J. Chem. Phys.*, 5320
Herbig, G. H. 1949, *ApJ*, 109, 109
Huber, K., & Herzberg, G. 1979, *Constants of diatomic molecules*, 240
Jonsson, J. 1994, *J. Mol. Spectrosc.*, 167, 42
Joyce, R. R., Hinkle, K. H., Wallace, L., Dulick, M., & Lambert, D. L. 1998, *AJ*, 116, 2520
Kaledin, L. A., McCord, J. E., & Heaven, M. C. 1995, *J. Mol. Spectrosc.*, 174, 93
Keenan, P. C. 1954, *ApJ*, 120, 484
Keenan, P. C., & Boeshaar, P. C. 1980, *ApJS*, 43, 379
Kiess, C. C. 1948, *PASP*, 60, 252
King, A. S. 1924, *PASP*, 36, 140
Lagerqvist, A., Uhler, U., & F, B. R. 1954, *Arkiv for Fysik*, 8, 281
Lambert, D. L., Smith, V. V., Busso, M., Gallino, R., & Straniero, O. 1995, *ApJ*, 450, 302
Langhoff, S. R., & Bauschlicher Jr, C. W. 1988, *J. Chem. Phys.*, 89, 2160
—, 1990, *ApJ*, 349, 369
Lauchlan, L. J., Brom Jr, J. M., & Broida, H. P. 1976, *J. Chem. Phys.*, 65, 2672
Lindgren, B. 1973, *J. Mol. Spectrosc.*, 48, 322
Little-Marein, I. R., & Little, S. J. 1988, *ApJ*, 333, 305
Littleton, J., Davis, S. P., & Song, M. 1993, *ApJ*, 404, 412
Littleton, J. E., & Davis, S. P. 1985, *ApJ*, 296, 152
Lowater, F. 1932, *Proc. Phys. Soc.*, 44, 51
—, 1935, *Phil. Trans. A*, 234, 355
McKemmish, L. K., Masseron, T., Sheppard, S., et al. 2017, *ApJS*, 228, 15
Merrill, P. W. 1922, *ApJ*, 56, 457
Murthy, N. S., & Prahllad, U. D. 1980, *J. Phys.B: At. Mol. Phys.*, 13, 479
Murty, P. 1980a, *Astrophys. J*, 240, 363
Murty, P. S. 1980b, *Astrophys. Space Sci.*, 68, 513
Petterson, A., Koivisto, R., Lindgren, B., et al. 2000, *J. Mol. Spectrosc.*, 200, 65
Phillips, J., & Davis, S. 1979a, *ApJ*, 229, 867
Phillips, J., Davis, S., & Galehouse, D. 1979, *ApJ*, 234, 401
Phillips, J. G. 1955, *PASP*, 67, 19

- Phillips, J. G., & Davis, S. 1979b, *The Astrophysical Journal*, 234, 393
- Phillips, J. G., & Davis, S. P. 1976a, *ApJ*, 206, 632
- 1976b, *ApJS*, 32, 537
- Piccirillo, J. 1980, *Monthly Notices of the Royal Astronomical Society*, 190, 441
- Plez, B., Van Eck, S., Jorissen, A., et al. 2003, in *IAU Symp.*, Vol. 210
- Richardson, R. S. 1931, *PASP*, 43, 76
- Sauval, A. J., & Tatum, J. B. 1984, *ApJS*, 56, 193
- Schoonveld, L., & Sundaram, S. 1974, *ApJ*, 192, 207
- Shankar, A., & Littleton, J. E. 1983, *ApJ*, 274, 916
- Shanmugavel, R., & Sriramachandran, P. 2011, *A&AS*, 332, 257
- Simard, B., Mitchell, S., Hendel, L., & Hackett, P. 1988a, *Faraday Discussions of the Chemical Society*, 86, 163
- Simard, B., Mitchell, S. A., Humphries, M. R., & Hackett, P. A. 1988b, *J. Mol. Spectrosc.*, 129, 186
- Smith, V. V., & Lambert, D. L. 1985, *ApJ*, 294, 326
- 1986, *ApJ*, 311, 843
- Sousa-Silva, C., McKemmish, L. K., Chubb, K. L., et al. 2018, *Phys. Educ.*, 53, 015020
- Sriramachandran, P., & Shanmugavel, R. 2012, *New Astronomy*, 17, 640
- Stepanov, P., Moskvitina, E., & Kuzyakov, Y. Y. 1988, *Spectrosc. Lett.*, 21, 225
- Suenram, R. D., Lovas, F. J., Fraser, G. T., & Matsumura, K. 1990, *J. Chem. Phys.*, 92, 4724
- Tanaka, T., & Horie, T. 1941, *Proc. Physico-Mathematical Soc. Japan*, 3rd Series, 23, 464
- Tatum, J. B., & Balfour, W. J. 1973, *J. Mol. Spectrosc.*, 48, 292
- Tennyson, J., Lodi, L., McKemmish, L. K., & Yurchenko, S. N. 2016, *J. Phys. B: At. Mol. Opt. Phys.*, 49, 102001
- Tennyson, J., & Yurchenko, S. N. 2017, *Mol. Astrophys.*, 8, 1
- Tennyson, J., Bernath, P. F., Brown, L. R., et al. 2009, *J. Quant. Spectrosc. Radiat. Transf.*, 110, 573
- 2010, *J. Quant. Spectrosc. Radiat. Transf.*, 111, 2160
- 2013, *J. Quant. Spectrosc. Radiat. Transf.*, 117, 29
- 2014a, *Pure Appl. Chem.*, 86, 71
- 2014b, *J. Quant. Spectrosc. Radiat. Transf.*, 142, 93
- Tóbiás, R., Furtenbacher, T., Császár, A. G., et al. 2018, *J. Quant. Spectrosc. Radiat. Transf.*, 208, 152
- Uhler, U. 1954a, PhD thesis
- 1954b, *Arkiv for Fysik*, 8, 295
- Uhler, U., & Åkerlind, L. 1955, *Naturwissenschaften*, 42, 438
- Uhler, U., & Åkerlind, L. 1956, *Arkiv For Fysik*, 10, 431
- Van Eck, S., & Jorissen, A. 1999, *Astronomy and Astrophysics*, 345, 127
- 2000, *A&A*, 360, 196
- Van Eck, S., Jorissen, A., Udry, S., et al. 2000, *A&AS*, 145, 51
- Van Eck, S., Neykens, P., Jorissen, A., et al. 2017, *Astronomy & Astrophysics*, 601, A10
- Weltner, W., & McLeod, D. 1965, *Nature*, 206, 87
- Wyckoff, S., & Clegg, R. E. S. 1978, *MNRAS*, 184, 127
- Zijlstra, A. A., Bedding, T. R., Markwick, A. J., et al. 2004, *MNRAS*, 352, 325